Zeitschrift: Schweizerische mineralogische und petrographische Mitteilungen = Bulletin suisse de minéralogie et pétrographie

Band: 66 (1986)

Heft: 3

Artikel: The Lake Nyos gas catastrophe (Cameroon) : a magmatological interpretation

Autor: Schenker, Franz / Dietrich, Volker J.

DOI: https://doi.org/10.5169/seals-50899

Schweiz. mineral. petrogr. Mitt. 66, 343–384, 1986

The Lake Nyos gas catastrophe (Cameroon). A magmatological interpretation.

by *Franz Schenker*[1] and *Volker J. Dietrich*[2]

Abstract

In the night of August 21, 1986 1746 people and a large number of animals died of suffocation from CO_2 rich gases emitted from a maar lake in NW-Cameroon. The gas burst occurred asymmetrically, uprooting the trees at the southern end of the lake approx. 30 m above water level. Animal cadavers were found to an elevation of 150 m above the lake.

The Nyos maar is a result of phreatomagmatic volcanism and probably less than 1000 years old. It may have formed from basaltic magma ascending along fault planes and intersecting water-filled fault systems. NW-Cameroon is a zone of very high precipitation (> 3 m/a). During the rainy season the three major fault systems (NE–SW, N–S and NNW–SSE) can easily be filled with meteoric water. The lavas and pyroclastics produced are primitive mantle derived basanites, ankaramites and alkalic basalts. According to oxide thermometry the Nyos basaltic lavas extruded with temperatures between 1020 and 950 °C. The lherzolitic and harzburgitic nodules carried up from the mantle in the magmas were equilibrated at pressures between 18 and 10 kbars (= 55 to 30 km depth) and temperatures between 900 and 1000 °C. The lherzolites contain Ti- and Cr-rich pargasite, which implies the presence of water in the upper mantle source.

In NW-Cameroon three areas of large magma reservoirs may be present at or below the crust/mantle boundary because of hydrothermal activity: Foumbot/Lake Manoum, Bamboui and Lake Nyos/Lake Wum. Most of the hot springs have high CO_2-concentrations close to solubility at atmospheric pressure. Their high Sr and Ba contents indicate a close relationship to the alkaline magmas.

Volcanic eruptions bring gas up from the interior of the earth crust and from the upper mantle. Primitive, alkaline magmas of basanitic, ankaramitic and basaltic composition are often accompanied by large amounts of volatiles, in particulary of CO_2, H_2 and CH_4. The origin of CO_2 in the magma reservoirs and in the hydrothermal systems is rather complex. We favour the hypothesis of mantle origin by the reaction: $CH_4 + 2\,H_2O = CO_2 + 4\,H_2O$. The production of CO_2 runs parallel with the generation of primitive alkaline melts by partial melting from a lherzolitic mantle source.

In Lake Nyos, the sediments together with a fault system at the southern end of the lake as well as the water itself seem to have acted as a gas trap. The gas burst was finally released by a minor earthquake, internal CO_2 overpressure or a water overturn of the CO_2-supersaturated bottom water during the rainy season.

Keywords: Volcanism, basaltic magma, volatiles, Lake Nyos, Cameroon.

[1] GEMAG AG, CH-6248 Alberswil, Switzerland.

[2] Institut für Mineralogie und Petrographie, ETH-Zentrum, CH-8092 Zurich, Switzerland.

1. Introduction

1.1. THE LAKE NYOS CATASTROPHE (AUGUST 21, 1986)

In the night from the 21 to the 22 August 1746 people and a large number of wild and domestic animals were killed by gases emitted from a maar-lake in NW-Cameroon (Fig. 1). The first reports of the catastrophe reached Switzerland on Sunday the 24 of August. The *Swiss Disaster Relief Unit* offered the authorities in Cameroon their help, and according to the wishes of President Bija the Swiss government set up a team to evaluate the possible assistance to be given and to try to explain the cause of the catastrophe.

On the 26 of August the Swiss team, composed of a logistical director, a medical doctor, a radio operator, a gas specialist, a geologist, and an advisor with knowledge of the local population and area, arrived in Cameroon. At this time, the danger of possibly lingering or still emitting gases was totally unclear, and to assure the safety of the team, it was not only necessary to bring analytical equipment but also alarm systems and gas masks.

Six days after the gas outbreak the only signs of what had happened were the fresh graves, animal's bodies, the stench of rotting meat and the silence because of the total absence of animal noises and bird songs. The fear of gas pockets in the valleys proved to be groundless. In spite of two days intensive searching in the whole area with gas detectors no great differences from the normal air composition could be measured (see Appendix: Gas Measurements). Hydrochemical and bacteriological field experiments on drinking water showed no chemical changes from that of drinking water outside of the stricken area; and the bacteriological measurements varied within the norms for the area.

After the return to the district capital Bamenda the *Swiss Disaster Relif Unit* gave the local authorities the following report:

- The air composition in the stricken area is normal and there are no remaining "gas pockets".
- The drinking water wells and reservoirs show no chemical anomalies and there is no measurable bacteriological increase due to contamination from cadavers.
- Neither the crops nor the food stores show any chemical contamination, they are all definitely edible.
- In the area there is no epidemic danger to the health of the surviving people or animals.

During the expedition to the catastrophe area and at Lake Nyos and Lake Wum several water, soil and rock samples were collected and from the area of the gas burst a geological map was made.

The samples were examined at the Institute for Mineralogy and Petrography of the ETH Zürich and in the laboratories of GEMAG AG. The chemical and

Fig. 1 Lake Nyos (August 30, 1986) facing southwest after the catastrophic gas burst. The clear waters have turned into a muddy suspension with reddish brown colors. The lake covers an area of approx. 1.4 km^2 and lays at an altitude of 1100 m. The steep cliffs in the foreground consist of pyroclastic deposits. On the opposite side of the lake granitic basement rocks are exposed. Photo Heldstab.

petrological studies should help to answer the many questions about the composition of the gases and the gas burst mechanism. The goal of this study is to provide as much data as possible in order to understand such catastrophic events. Only on this basis a prognosis of future events is possible, lives and property can be saved.

1.2. THE DAMAGE SITUATION

The area involved in the catastrophe lays between the villages of Nkambe and Wum on the ringroad to Bamenda (Fig. 2). The size of the devastated area based on reported deaths and animal bodies found can be estimated at 300 km^2, Lake Nyos (10°17′55″E/6°27′15″N) probably being the southernmost point and Fang the northernmost. The village of Bum (or Subum) and Kumfuhtū, which are approximately 24 km apart, are the eastern and western boundaries.

The area, which lays between rain-forest and steppe, is composed of grass- and bush-covered hills and crosscut by flat valleys overgrown with tropical vegetation. In the valleys farmers settled in small villages, and in the hills live

nomadic cattle raisers (Fulani) who have a number of scattered camps from which they watch their cattle. The surviving Fulanis have been, as far as property is concerned, much more hit by the catastrophe because their only property, the herds of cattle, were also killed. The fruit trees and crops of the farmers suffered no damage.

Before the catastrophe occurred, according to the information provided by survivors, there were no strange smells, dead fish or earthquakes. However, on August 21 between 8:00 and 10:00 p.m. there were three muffled thunder-like noises.

The population of Subum reported that the gases smelled like rotten eggs and gunpowder although the population of the villages closer to the disaster made no such reports. They woke up on Friday morning, August 22, feeling very tired, were disoriented with differing periods of unconsciousness and had some paralysis. Many complained of difficulties breathing, vomiting and had chemical burns on their skin, although in most cases the burns were only on one side of the body. All of the survivors reported that on Friday all of the insects were gone. The helicopter pilots of the Helimission reported on Saturday morning that it appeared as if the deaths of the people and animals happened very quickly because the bodies were found in houses, in the squares and along the paths as if they had been stopped in the process of doing their normal activities.

It can be determined from the reports that the victims lost consciousness very quickly and then after a few minutes died by suffocation. The smells point to hydrogen sulfide (H_2S) and sulfur dioxide (SO_2) gases, which are already noticible by smell in small concentrations (for H_2S: 0.5 ppm, for SO_2: 100 ppm). The chemical burns show that in the gas cloud acids in suspension (e.g. HCl, H_2SO_4) probably have been present.

1.3. THE COMPOSITION OF THE LETHAL GASES

Local indications:

At the end of August, it was no longer possible along the shores of Lake Nyos or in the devastated area to detect gas anomalies in the atmosphere or in the water. The composition of this surface water was similar to that of rain water (Tab. 6 in Appendix). In order to get an estimate of the nature and composition of the gas it is necessary to rely upon existing indications and comparisons with similar catastrophic events.

Medical indications:

- The main cause of death was lack of oxygen. People and animals lost consciousness quickly and died of suffocation.
- Survivors and dead bodies showed burns on unprotected skin, the lungs were infected and inflamed.

- The gases were heavier than air. This is shown by the fact that cadavers were found mainly in the valleys, the village Higher Nyos, located approx. 300 m above the lake, was spared by the catastrophe. The village furthest from the outburst where dead were reported marks a topographical low-point (Fig. 2).
- Thus, the only possible gas, which could have caused such a rapid and deadly dissipation must have been carbon dioxide. A 10–20 per cent mixture of CO_2 with air is potentially lethal.
- The gases must have been relatively cold, only in the immediate area of the outburst were burns of trees and flora recognized.
- The role of carbon monoxide as lethal gas can be ruled out. None of the dead showed any replacement of hemoglobin (reports from the American team of Doctors).

Geological indications:

- Lake Nyos represents a maar, although its shape is slightly atypical. The outburst of lethal gases showed an asymmetrical pattern which indicates that the gases were derived from a gas trap below the lake sediments connected with the NW–SE striking fault system at the southern part of the lake (Fig. 3 and 4). Because of its morphology with steep cliffs along the shores, the Nyos maar might have a young age (< 1000 years) and thus the area be magmatically still active. The peridotitic nodules within the alkali-basaltic pyroclastics are the proof of a deep seated transport system.
- Numerous thermal springs surround the volcanic centers of the Cameroon line. Most of the waters have high contents of carbon dioxide close to the saturation level at one atmosphere pressure (MARÉCHAL, 1976). In the vicinity of Lake Nyos two thermal springs have been reported (Fig. 2).

Similar gas catastrophes:

- In August 1984 a similar gas burst from Lake Manoun near the village of Foumbot (80 km SE of Nyos) led to instant death of 37 people. This lake is formed by two craters and placed almost in the center of the Foumbot crater field (TCHOUA, 1983), in which at least 40 scoria cones and maars were produced probably during the past 1000 years. Earthquake activity (e.g. the Magba earthquake in September 1983, STUART et al., 1985) and thermal springs south of Foumbot (with 29 °C and 700 mg/l CO_2, MARECHAL, 1976) indicate that this volcanic field is still active and an area of high risk. The gas analysed from deep water from Lake Manoun consists mainly of CO_2 (97 vol.%) and minor CH_4 (ca. 2 vol.%). Oxygen and carbon isotopic compositions indicate a volcanic origin with long-term exhalation from the vents within this crater lake (SIGURDSSON et al., 1986).
- VERSCHUREN (1965) reported gas measurements on holes in the East African Rift Zone (Zaire). This volcanic zone is a large analogy to the Cameroon

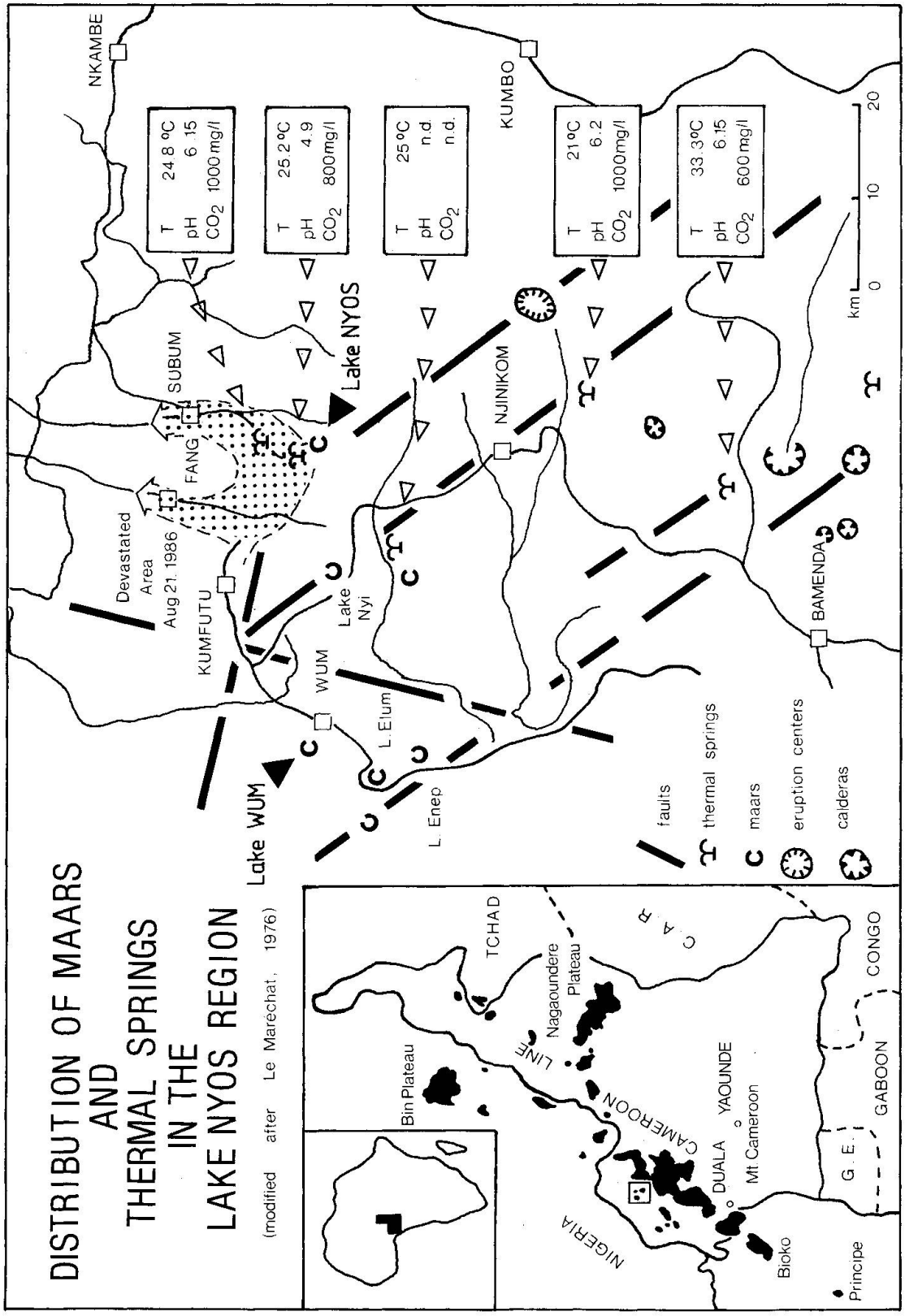

Fig. 2 Locality map of the Wum-Nyos region (NW-Cameroon).

line. CO_2 is the major component of the gases. Numerous animals died of suffocation in the so called Masutus (gas holes).

Similar results on volcanic gases have been obtained from many volcanic fields all over the world. In general CO_2 rich gases (mofettes) have been observed as post-eruptive exhalations from the vents. Normally they are harmless and dissipate directly into the atmosphere. In the case of the Cameroon catastrophe the gases were trapped below the sediments and within the water of the maar lake.

We conclude from the collected evidence that the killer gas of Lake Nyos was for the most part carbon dioxide. The burns only on trees restricted to the close vicinity of the outburst point to coexisting hydrogene gas which reacted spontaneously with the air causing an explosion. Hydrochloric acid, methane and hydrogen sulfide were minor accompanying components in the gas burst and probably reacted with air to form acids etc.

1.4. GEOLOGICAL OBSERVATIONS, MAPPING AND SAMPLING

The devastated area (Fig. 2) lays on the northwestern edge of the active chain of alkaline volcanoes (Cameroon Line) which has been active since Oligocene time. Lake Nyos as well as Lake Wum and a few other small lakes in the area around the town of Wum are classical maars with diameters between 300 m and 2 km. Such maars or diatremes are formed by phreatomagmatic eruptions of basaltic magmas. The area of approx. 600 km^2 between Lake Nyos and Lake Wum has several outstanding geological features. The basement rocks consist mainly of Precambrian rapakivi-type granites, gneisses and schists and are penetrated by three major steeply dipping fault systems. In most places, the basement rocks are deeply weathered producing the typical landscape with smooth hills and valleys. Between Wum and Nkambe the basement is partly covered by alkali-basaltic and ankaramitic lava flows.

The villages of Subum and Fang are situated in valleys which are filled with Alluvial deposits. Pebbles in the rivers and creeks are mostly porphyritic alkali feldspar granites.

Lake Nyos lays on a plateau at 1100 m altitude and approx. 300 m above the villages. Its waters originate only from a small area of ca. 6 km^2. The grade of the incoming creeks and the amount of inflowing waters is small. The drainage to the north runs over a pyroclastic barrier. The subaerial as well as the subaquaeous eastern and western crater walls are steeply downward-sloping, in the south four inflowing creeks have formed small alluvial fans (Fig. 3).

The following geological observations could be made:

- Except in the south the crater walls are very steep and consist for the most part of granitic rocks which are in several places hydrothermally altered and soft (Fig. 3). These granites are crosscut by numerous veins which, in their cen-

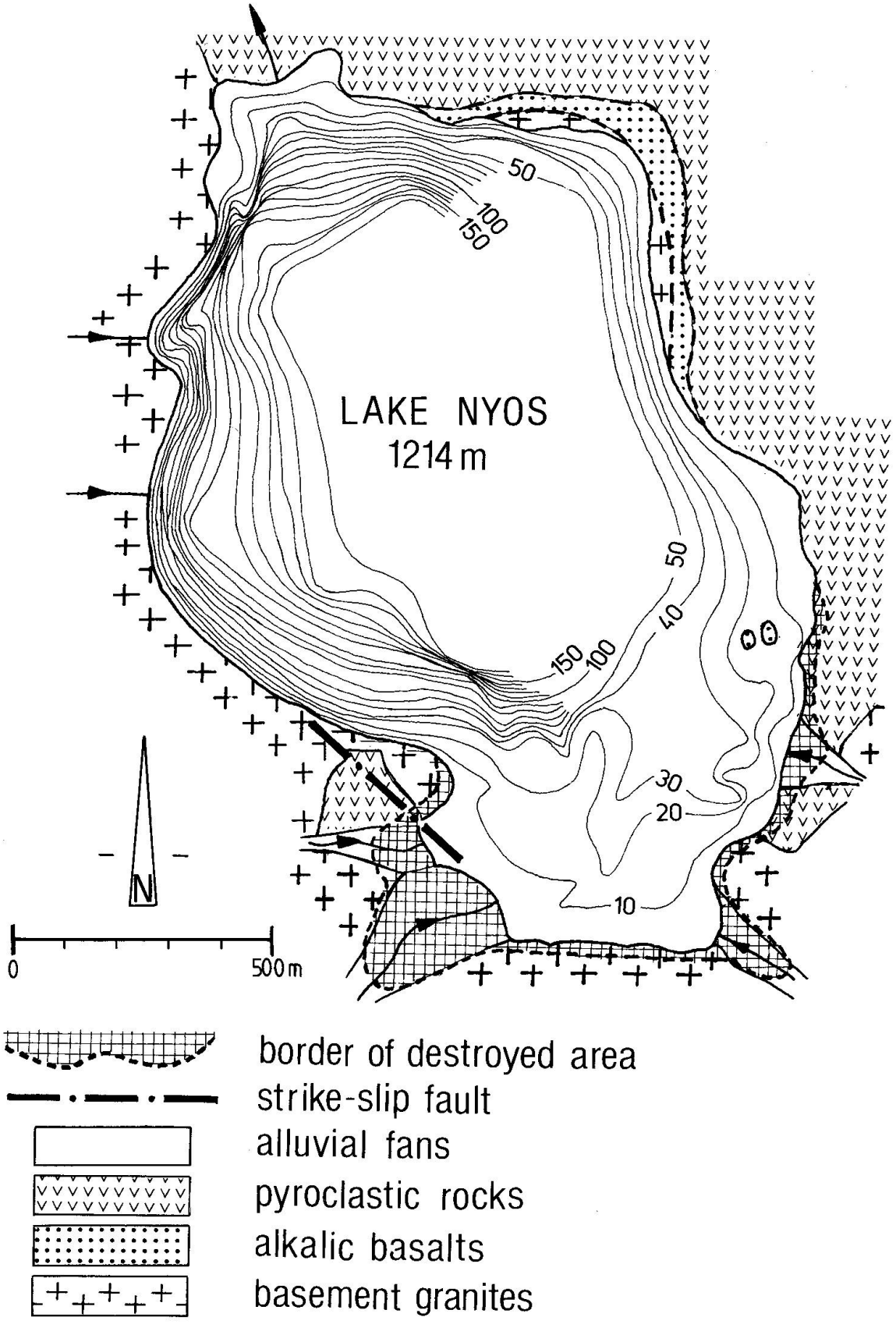

Fig. 3 Geological map of Lake Nyos. Depth contours: HASSERT (1912).

ters, consist mainly of fine-grained quartz accompanied by clay minerals and gibbsite.

- The alkalic olivine basalt appears as a small flow, overlaying directly the granitic basement in the northeast.

- At three locations pyroclastic deposits are exposed (Fig. 1, 3 and 5). To the northeast of the lake the tuffs are horizontally bedded, in the southwest they are tectonically realigned along a NW–SE striking fault (Fig. 4). The total thickness of the tuff beds reaches 20 m. They are composed of poorly sorted thin-bedded layers with 2 to 80 cm in thickness, and locally show cross-bedding and antidune structures. However, around Lake Nyos a real tuff ring could not be established. Nearly all blocky shaped basaltic clasts are highly glassy and nonvesiculated. They contain white broken pieces up to a few cm in diameter of basement granites and gneisses. The larger and partly rounded clasts (up to 30 cm) are mainly green peridotitic nodules, rimmed by black glass-rich basaltic crusts. The peridotitic nodules are weathered to different degrees and occur abundantly in the alluvial deposits. There, it is not clear if these nodules were transported by the creeks or if they represent ejecta from recent maar eruptions.

- In spite of intensive searching, it was impossible to find rising gas bubbles in the lake or in cracks of the surrounding rocks.

- No evidence of recent or historical fumarolic activity (e.g. in the form of sulfur minerals, zeolites, salts or carbonates) has been found.

Fig. 4 Strike-slip fault striking NW–SE at the SW end of Lake Nyos. To the right realigned tuff beds (August 30, 1986).

Fig. 5 Lake Nyos on August 30, 1986 facing south. The northern spillway shows no signs of the flood wave (see undisturbed tree at the edge of the waterfall), although the lethal gas cloud must have moved over this area. On the left side (eastern shore) and in front the lake borders pyroclastic deposits which overlay the granitic basement and are slightly inclined towards the lake. In the far background the white line marks the upper limit of the destruction caused by the asymmetrically oriented flood wave. Photo Heldstab.

- In the northern area and in the area of the stream draining there was no evidence of a flood wave (Fig. 5). Residents reported that the drainage started again three days after the outburst.
- Only in the area along the southern shoreline trees were uprooted and stripped to an altitude 30 m above the lake (Fig. 3 and 5). Along the boundary to the undamaged vegetation the trees lay upwardly against the slope, the rest of the trees lays downwards towards the lake.
- Several trees with fresh fruit showed very thin burn marks on the stems and leaves.
- Animal cadavers were only found to an elevation of 150 m above the lake.
- The concentration of CO_2, H_2S, CO, SO_2, HCl, CH_4, and H_2SO_4 were all within the normal ranges. The O_2 concentrations in the air were 21 %.

2. Magmatological considerations in relation to the genesis of the lethal gases

2.1. THE VOLCANIC CAMEROON LINE

Lake Nyos, Lake Wum and numerous other small craters in NW-Cameroon belong to a linear chain of alkaline volcanoes which extend from the islands of

Pagalu, São Tomé, Principe, Bioko and Etinde (Gulf of Guinea, South Atlantic) into Cameroon and Nigeria over a total distance of 1600 km (Fig. 2). This SW–NE striking volcanic line is linked with several large fault systems which penetrate the Precambrian West African basement. The age of the volcanic activity started about 35 ma (with maximum ages of igneous activity of about 65 ma) at Oligocene time and continued until today with the 1982 eruption at the largest volcano Mt. Cameroon (FITTON et al., 1983, FITTON and DUNLOP, 1985).

Speculations that the Cameroon volcanic chain might represent a hot-spot trail are unlikely because of the age distribution of volcanic activity. Oligocene and Miocene as well as recent activity has occurred through the entire length of the volcanic chain (FITTON and DUNLOP, 1985).

It is more likely an incipient rift and might be connected with the development of the Cretaceous Benue trough starting with the breakup of Africa and South America by lithospheric stretching as one arm of an R R R triple junction (BURKE and DEWEY, 1973).

In any case, the Cameroon line represents a surface expression of a deep seated fault system, probably coupled with a thermal anomaly in the asthenosphere which causes partial melting over a narrow but long distance. The uncoupling of the Benue trough from the Cameroon line and movement into its present position may be explained by a 7° anticlockwise rotation of the lithosphere about a pole in Sudan relative to the asthenosphere (FITTON and DUNLOP, 1980 and 1983). However, the upwelling of the mantle with the generation of magmas may be the reason for the formation of the horst-graben system in Cameroon.

Since Paleocene time the magmatic activity of the Cameroon line occurred along a deep seated continuation of a South Atlantic fracture zone into the West African continent. This fracture zone acted in a more or less steady state with tensional features but little vertical and horizontal displacements.

The base of the volcanic islands of Pagalu, São Tomé, Principe, and Bioko is mainly normal oceanic crust and probably formed during Upper Cretaceous and Tertiary. The volcanic edifice of Mt. Etinde and Mt. Cameroon rests on Quarternary continental margin sediments which extend to the NE into the Tertiary sandstones and slightly folded Upper Cretaceous shales in the Bakunde Plain (GÈZE, 1943). From there to the NW the volcanics overlay mainly crystalline basement made up of granitic gneisses and mica schists which have been intruded by alkaline ring complexes (gabbro–syenite–granite) of Paleocene to Eocene age (CANTAGREL et al., 1978; LASSERRE, 1978).

The volcanic zone is at the latitude 4°N of Mt. Cameroon approximately 50 km wide and widens towards the NE to about 80 km. It splits at 7°N and continues N into the Bice Plateau and Madara Mts. and towards E into the Ngaoundéré Plateau.

According to GÈZE (1943) most of the volcanic fissures and centers of eruptions are linked with smaller NNE–SSW striking fault systems. In general, along the whole Cameroon system a (stratigraphic) relative age distribution of the volcanic pile has been mapped. Volcanic activity started with flows, pyroclastic flows and breccias in Oligocene time. The material consists mainly of trachyandesites and trachybasalts as well as of normal alkaline basalts and a few basanites. Within the larger volcanoes of Mt. Cameroon, Mt. Manengouba and Mts. Bamboutos, this Série Noire Inférieure (GÈZE, 1943) is overlain by larger masses, flows, pyroclastics, and necks of trachytic and phonolitic composition (Série Blanche). The youngest volcanic lavas forming the tops of Mt. Cameroon (Point 4070 m), and Mt. Manengouba are alkalic basalts and basanites (Série Noire Supérieure). Besides the larger composite volcanoes, hundreds of small basaltic scoria cones and maars exist aligned along fissures and fault zones. Their ages might range from approx. 1 ma until today.

According to the topographical map (1:100000) and to the work of MARECHAL (1976) and TCHOUA (1983) at least six major volcanic craters and a dozen smaller scoria cones and maars occur in the region between Lake Wum, Lake Nyos, Bamenda and Kumbo. These eruptive centers were formed at intersections of feeder dikes striking more or less in the NE–SW direction of the Cameroon line with a NW–SE trending major fault system (Fig. 2).

From the size and shape of the larger volcanic craters and of the smaller crater lakes it seems reasonable to interpret these centers as products of phreatomagmatic eruptions. However, the ages of the eruptions remain uncertain and at the moment an estimation can only be made by the morphology of the surrounding crater walls and pyroclastic deposits. Steep crater walls with sharp edges (e.g. Fig. 1) are exposed at the lakes of Nyos, Enep, Nyi, Elum, Benakumba, and Bambuluwe (Fig. 2). Thus, these craters may have been formed within the past one thousand years, while Lake Wum, for example, exhibiting smooth, flat surroundings seems to be older.

2.2. PETROLOGY OF THE LAKE NYOS ALKALIC BASALTS AND PYROCLASTICS

The pyroclastic deposits at Lake Nyos show typical volcanologic and petrographic features which are equivalent with those described from the classical maars in the Eifel (Germany) or in the Massif Central (France) by LORENZ and ZIMANOWSKI (1984) and LORENZ (1986). At Lake Nyos (Fig. 3) the poorly sorted ashes, lapilli and bombs form up to 20 m thick pyroclastic deposits. The bedded ashes show in several localities cross-bedding and may be explained by a series of phreatomagmatic eruptions which took place during days.

Cauliflower shaped lapilli and bombs are also present. These textural features have been explained as due to interaction of the hot magma with meteoric water within fault zones. The latter process seems to be the cause for the phrea-

Tab. 1 Mineralogical characteristics of basaltic clasts, alkalic basalt (Lake Nyos) and ankaramite (Nkambe); for mineral chemistry see appendix, tables 3A–F).

	LN7 basalt. clast	LN 6 alkalic basalt flow	NK 2 ankaramite
Olivine:			
Phenocrysts		core:Fo 83–82, rim:Fo 78–77	core: Fo 84, rim: Fo 77
Microphenocrysts	Fo 87	Fo 77	Fo 77
Clinopyroxene:	not detected	TiO_2: core 4.2–4.1 rim 4.6–4.3	c: 5.4–4.6 r: 3.8–3.1 wt.%
Phenocrysts		xMg (Fe2+) 0.83–0.81	xMg (Fe2+) 0.84–0.81
Microphenocrysts		,, 0.78	,, 0.81
Plagioclase:			
Phenocrysts		core: An 60–58, rim: An57	An 74–65
Microphenocrysts	An 16–18 ?, An 64	An 53–45	An 60–50
Anorthoclase:	not detected		
Microphenocrysts		An21/Ab63–61/Or16–18	An3–10/Ab84–76/Or13–18
Alkali feldspar:			
Microphenocrysts:	? Xenocrysts Or84, Or 92–93	not detected	An 9–5/Ab36–33/Or54–62
Spinel in olivine:		xMg Spinel 0.34–0.31	xMg Spinel 0.64–0.55
		Cr_2O_3: 18–17 Al_2O_3: 16.5–14.9	Cr_2O_3: 14.8–11.8 Al_2O_3:
Ulvospinel:	not measured	0.54	0.67–0.47 44.7–34.4 wt.%
Ilmenite:	not measured	0.68	not detected

Glass:	select. pyroclast. glass		glass in olivine	groundmass glass	not measured
SiO_2 wt%	48.8	48.1	52.74	51.3	
TiO_2	2.78	2.99	1.58	2.65	
Al_2O_3	18.48	15.29	15.12	18.0	
FeO tot	9.00	12.89	4.59	7.4	
MnO	0.16	0.29	0.09	0.16	
MgO	3.84	6.37	5.35	3.8	
CaO	12.13	5.86	12.07	8.7	
Na_2O	3.83	3.00	4.70	5.25	
K_2O	1.33	2.43	2.31	2.3	
NiO	0.04	0.04	0.00	0.00	
Total	100.40	97.35	98.55	99.56	
Mg/Mg+Fe (tot)	0.43	0.47	0.68	0.48–0.44	

tomagmatic eruption (LORENZ, 1979 and 1986). This interpretation is consistent with the textural evidence observed in the groundmass glass, microphenocrysts and xenolithic material of the clasts and cauliflower bombs. The groundmass glass (Table 1) is very dense and has a very low vesicularity (Fig. 6). Olivine and plagioclase show excellent quench textures. These features can only be explained by a mechanism of rapid undercooling of hot basaltic melts by cold groundwater.

The mineral and glass compositions of the Lake Nyos basaltic clasts and of the alkali-basaltic lava flow have been summarised in Table 1. It is important to note that the quenched olivine and plagioclase microphenocrysts are in equilibrium with the glass and are more primitive than those in the lava flow. The composition of the glass in the clasts is slightly variable. However, the average glass composition is almost identical with the bulk composition of the lava flow (Appendix, Table 4). The small albite-rich plagioclase and alkali feldspar grains which have been detected in the dense glass may be due either to xenolithic material from the granitic basement or to quenching under disequilibrium conditions. In addition, Table 1 contains data of a typical ankaramitic lava flow near Nkambe (Fig. 8).

The xenolithic material is made up of two populations: one group consists of gneiss, schists and granitic fragments with entirely sharp angular shapes and a lack of any contact metamorphic influence (Fig. 6), and the other more rounded group is made up of peridotitic and gabbroic material. The peridotite inclusions dominate and reach dimensions up to 30 cm in diameter. Rounding or contact metamorphic effects of the inclusions are very rare. Reaction mineral assemblages (coronas) only occur around gabbroic components which means that the basaltic melts were in contact with cumulate material, probably at greater crustal depth.

Tab. 2 Mineralogical characteristics of lherzolitic nodules from lake Nyos alkalic basalt pyroclastics; for mineral chemistry see appendix, tables 3A–F.

	LN P3 lherzolite	LN P4 lherzolite
Olivine:	Fo 91–90	Fo 91–90
Orthopyroxene:	xMg (Fe tot) 0.91 Al_2O_3: 2.2–2.4 wt.%	xMg (Fe tot) 0.92–0.91 Al_2O_3: 4.05–4.25 wt.%
Clinopyroxene:	xMg (Fe tot) 0.92–0.91 Al_2O_3: 5.6 wt.%	xMg (Fe tot) 0.91 Al_2O_3: 6.8–7.3 wt.%
Spinel:	xMg Spinel 0.83–0.82 Cr_2O_3: 10.6 Al_2O_3: 56.5 wt.%	xMg Spinel 0.82–0.81 Cr_2O_3: 8, Al_2O_3: 59.9 wt.%
Pargasitic Amphibole:	---	xMg (Fe tot) 0.89 TiO_2: 2.9–3.3 wt.% Al_2O_3: 15.4–14.4 wt.%

Table 2 summarizes the mineral composition of the amphibole bearing peridotitic nodules.

According to the normative mineral composition based on bulk chemical analyses (Table 5 Appendix) these nodules exhibit harzburgitic and lherzolitic compositions. Main constituents are olivine (Fo 91–90 Table 2 and 3A) and orthopyroxene (xMg 0.92–0.91). Spinel is present up to approx. 6%. The spinel lherzolites, in addition, contain interstitial amphibole (Fig. 9). The higher amounts of Al, Ca and Ti in the pyroxenes and spinels (Tables 3B, 3C and 3E) are also reflected in the bulk chemistry.

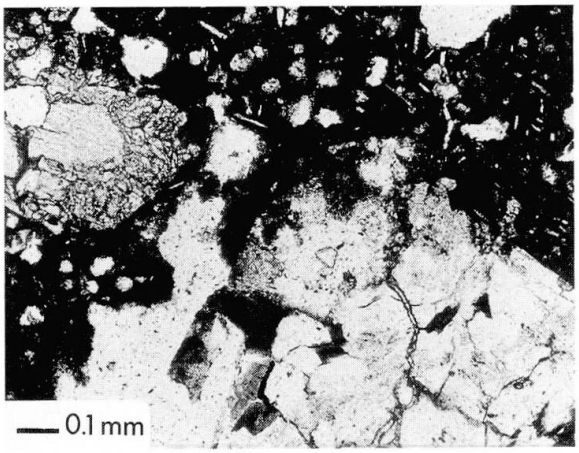

Fig. 6 Glassy alkali-basaltic clast (LN7) from the pyroclastic deposits at the southern end of Lake Nyos. Groundmass glass with minor vescicles and quenched microphenocrysts of plagioclase, olivine and alkali feldspar (Table 1). Left side: Plagioclase xenocryst rimmed by a corona of clinopyroxene. Lower part: Biotite-granite fragment without reaction rim.

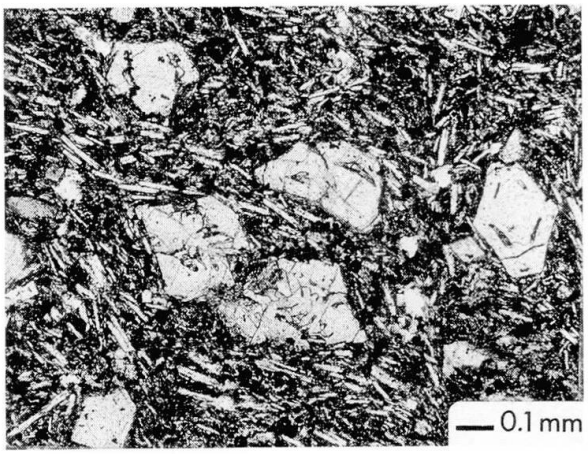

Fig. 7 Alkalic olivine basalt (LN6) form the eastern shore of Lake Nyos. Olivine phenocrysts (Fo83–77) with elongated glass inclusions exhibiting quench textures. Trachyandesitic groundmass glass (Table 1) contains microphenocrysts of olivine (Fo77), plagioclase, anorthoclase, ulvospinel and ilmenite.

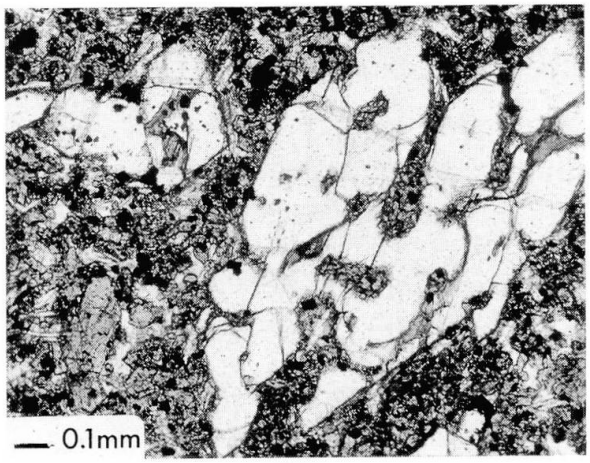

Fig. 8 Ankaramite. Lava flow approx. 30 km west of Nkambe. Partly resorbed olivine (Fo84–77) phenocrysts with minute spinel inclusions. The groundmass consists of a granular eutectic mixture of clinopyroxene, plagioclase, anorthoclase, alkali feldspar and ulvospinel (Table 1).

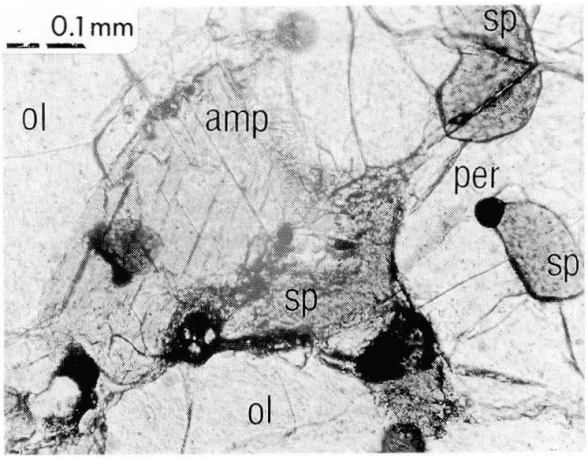

Fig. 9 Interstitial pargasitic amphibole (amp) surrounded by olivine (ol), spinel (sp) and perowskite (per) in the spinel lherzolite nodule (LNP4) from Lake Nyos.

2.3. GEOCHEMISTRY OF ALKALIC BASALTS, PYROCLASTICS AND PERIDOTITIC NODULES

Volcanic eruptions release gas from the interior of the earth crust and from the upper mantle. The emissions mainly consist of water, carbon dioxide, molecular hydrogen (BARNES and MCCOY, 1979; SATO, 1978) as well as of methane (DEUSER et al., 1973), ammonia, hydrogen sulfide, chlorine, and others. Although all gases undergo recycling in the crust and atmosphere (biological and sedimentary cycles), they must have originated in the earth mantle. There is much evidence (e.g. in meteorites) that the earth required much of its carbon in form of hydrocarbons, which are stable gas phases at high pressures.

Primitive silica-undersaturated alkaline magmas of basanitic, ankaramitic and olivine basalt compositions are often accompanied by large amounts of volatiles, in particularly by CO_2, H_2 and CH_4. Experimental evidence (RINGWOOD, 1975) indicates, that such magmas must have originated in the deeper parts of the mantle (80 to 150 km) as the result of small amounts of partial melting from garnet lherzolite. The degree of partial melting is dependent on pressure and volatile content of the system.

This shows, that there is an intimate relationship between volatiles and generation of alkalic melts. In addition, the uprising melts provide an ideal transport media for the dissolved gases.

Petrologically, the alkalic volcanic rocks of the Cameroon line range in composition from basanites and ankaramites through normal alkalic basalts and trachybasalts to trachytes, phonolites and alkali-rhyolites. Selected bulk chemical compositions of basaltic lavas and pyroclastic rocks from the Nkambe – Lake Nyos – Lake Wum – region are given in Table 4.

The voluminous part of the Cameroon volcanics consists mainly of normal and undersaturated alkalic basalts (Fig. 10) with rather low abundances of Na_2O (3.36 ± 0.72 wt.%) and K_2O (1.47 ± 0.42 wt.%).

Most of the alkalic rocks are nepheline-normative, a certain percentage crosses the olivine-plagioclase-diopside plane (the thermal divide in the basaltic tetrahedron) and are hypersthene-normative and a few are even quartz-normative.

On the basis of normative mineral compositions MIYASHIRO (1978) classified the alkalic volcanic rock series into three major categories: One common rock association, designated as "Kennedy-trend", starts from weakly nepheline-normative alkali olivine basalts, rich in potassium and sodium, and shows increasing normative nepheline with advanced differentiation to reach phonolitic composition. These rocks, which include trachybasalts, trachyandesites and trachytes typically are found in plateau basalts along continental margins and within many oceanic islands (e.g. Gough and St. Helena).

In contrast, other rock series designated as "Coombs-trend" starts from hy-

persthene normative basalts and follows the direction to hypersthene and quartz bearing rocks within the basaltic tetrahedron of YODER and TILLEY (1962) to reach comenditic compositions. These series typically include hawaiites and mugearites, thus trachybasalts and trachyandesites are richer in sodium and poorer in potassium than those within the "Kennedy-trend".

As combinations of Kennedy- and Coombs-trends, alkalic volcanic rock associations occur which start from primitive nepheline-normative alkalic olivine basalts, ankaramites and basanites, cross the low pressure thermal divide (olivine-diopside-plagioclase plane in the basaltic tetrahedron), reach hypersthene normative and finally quartz-normative rocks. MIYASHIRO assumed that these "Straddle-type" associations may have been differentiated at pressures above 10 kbar and under some hydrous or oxidizing conditions where the olivine-plagioclase-diopside plane is no longer a thermal divide. Crystallisation of low-silica minerals such as amphibole, magnetite and apatite may be the means of producing such trends. These alkalic trends occur in many places within stable continental environments as well as in oceanic islands (e.g. Tristan da Cunha) and aseismic ridges (e.g. Walvis Ridge: DIETRICH et al., 1984).

In our opinion, the diversity of the alkalic rocks and the appearance of the various differentiation series is dependent on three major factors: (1) the amounts of alkalis and hygromagmatophile elements, especially K, Rb, Sr, Ba and light rare earth elements (LREE) as well as on the amount of Ti and Fe in the parental magmas, (2) the depth of fractional crystallisation and, (3) the amount of water present in the parental magmas.

Titanium seems to be a very important element controlling the differentiation. It occurs in oxides, which appear in cumulates and gabbroic intrusives in many alkalic volcanics, but also to a major extent in clinopyroxenes and amphiboles. The stability field of the Ti-bearing silicates and oxides are highly dependent on oxygen fugacity, water and relatively high pressures (MERILL and WYLLIE, 1974). As far as we know, basanites, ankaramites and high-Mg alkalic olivine basalts cover a large field of primitive compositions and most probably parental alkalic melts.

In order to derive the various differentiated alkalic rocks in the Cameroon volcanics, we hypothesize complex differentiation processes starting from basanitic rocks and involve crystal fractionation, crystal accumulation, hybridization, mixing and mingling. These processes are based on petrographic observations as well as on mineral and bulk rock chemistry of all rock types. Mathematical modelling has been used by DIETRICH and CARMAN (in preparation) to test this hypothesis.

The model shows that a trachytic melt can be produced directly from a primitive ankaramitic melt by fractionation of large amounts (> 50 vol.%) of apatite-bearing, amphibole-rich, olivine, clinopyroxene, plagioclase, and magnetite cumulates. Indications of such a differentiation process for the Cam-

eroon volcanics is given by petrographic evidence in many alkalic basalt lavas which carry relicts of these cumulates. Besides plagioclase, clinopyroxene and magnetite often pargasitic to kaersutitic amphibole occurs (MESCH, 1916, JÉRÉMINE, 1943, GOUHIER et al., 1974).

The same minerals appear in the intermediate trachyandesites (hawaiites). However, there they are corroded and surrounded by reaction assemblages which indicate disequilibrium with the host rock. The groundmass often has

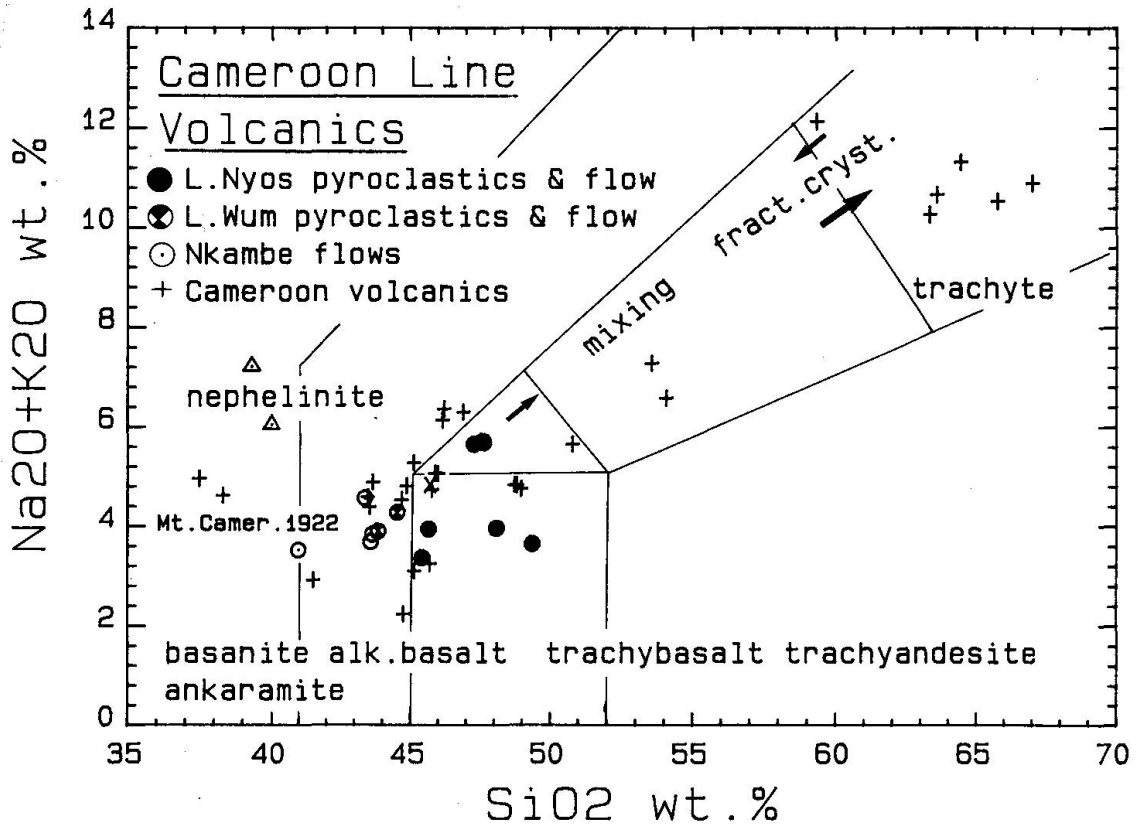

Fig. 10 The total alkali silica (TAS) diagram showing the alkaline volcanic rock associations of Western Cameroon. The major part of the lavas consists of alkalic basalt, basanite and ankaramite. The trachytes are produced by fractionation of amphibole bearing cumulates from the basanites. The intermediate trachybasalts (mugearites) and trachyandesites (hawaiites) are explained by complex processes of mixing (mingling and hybridization of cumulates). Exceptions are the nephelinites from Etinde (GÈZE, 1943).

trachytic compositions. For these reasons, most of the intermediate alkalic volcanics are regarded as mingling products of evolved trachytic melts with xenolithic (cumulitic) material. The origin of the trachybasalts is more complex and involves magmatic processes of fractional crystallisation, hybridization of cumulates and mixing with evolved melts (DIETRICH and CARMAN, in preparation).

Besides the chemical characterization, Fig. 10 shows the scatter of composition of the Lake Nyos pyroclastics compared to the composition of the lava

flows from the Nyos- and Wum-maars. The effect is due to contamination with granitic, gneissic and peridotitic material.

In Fig. 11 (MgO/Ni variation diagram) the contamination with peridotitic nodules in the pyroclastic material is clearly visible. Ni is highly enriched in the mud and soil samples from the southern end of Lake Nyos. In addition, the trend of fractional crystallisation with a linear negative correlation from basanite and ankaramite to trachyte and nephelinite is indicated by heavy black arrows.

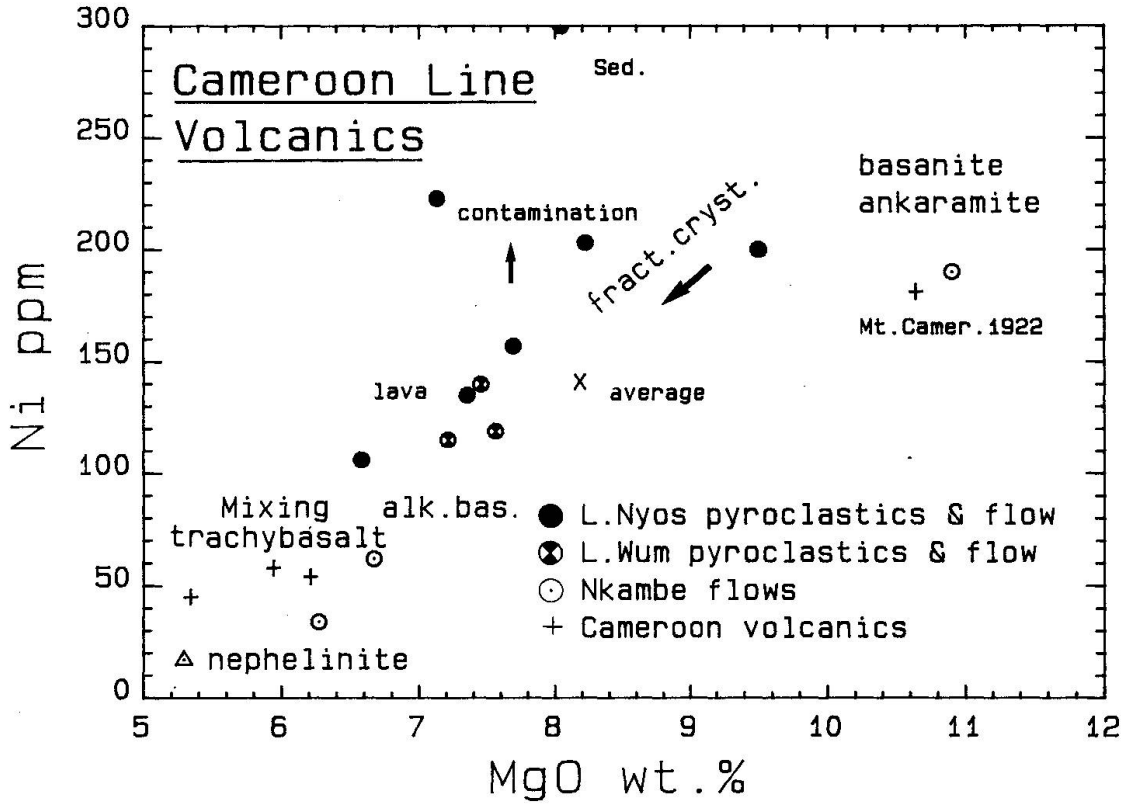

Fig. 11 MgO versus Ni indicating the intensive contamination of the Lake Nyos basalts with peridotitic material. Data from Mt. Cameroon lavas (FITTON et al., 1983), from other Cameroon lavas and nephelinite (FITTON and DUNLOP, 1985).

The trace element variation in the Cameroon alkalic volcanics is demonstrated only in the Zr/Y-variation diagram (Fig. 12). These strongly incompatible elements shall illustrate the genetic relationship between the primitive basaltic rocks and the evolved trachytes and nephelinites. In general, the ratios throughout the Cameroon lavas are the same indicating an origin from very similar parental melts. Exceptions are the basaltic pyroclastics and lavas from Lake Wum and the pyroclastics from Lake Nyos. The higher yttrium contents

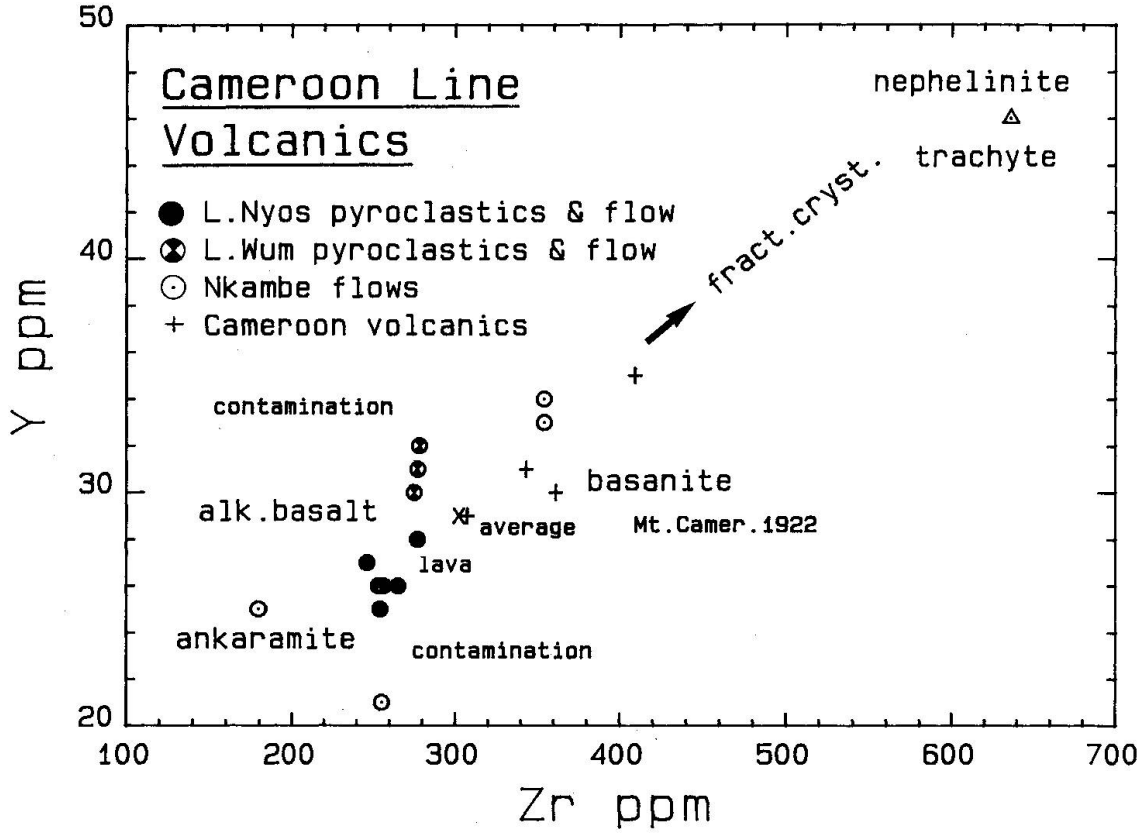

Fig. 12 Zr/Y variation diagram. Heavy arrow indicates the trend of fractional crystallisation.

in the Wum basalts indicate contamination with the Y-rich rapakivi-type granites while the lower yttrium contents in the Nyos basalts can be explained by contamination with peridotitic material. The absolute enrichement of Y and Zr (at a same ratio as the other volcanics) in the 1922 Mt. Cameroon basanite cannot be explained from our data.

From the last diagram as well as from the absolute trace element contents (Table 4) it seems evident, that fractional crystallisation, mingling and mixing are very similar throughout the entire Cameroon line. These processes must have taken place at different levels in the crust. The occurrence of lherzolitic and harzburgitic nodules in the alkalic basalts, basanites and ankaramites clearly indicate an upper mantle origin of these lavas. Pressure and temperature conditions will be discussed in the appendix.

The CO_2 and S data given in Tables 4 and 5 are shown in Fig. 13. No correlation exists between CO_2 and S. The values for CO_2 in the peridotites are small and overlap with those in the basalts and the ankaramite. The granites have similar values. However, much higher values occur in one pyroclastic sample (analysis not given in Table 4) and in the volcanic soil samples. The latter contents can be explained by infiltration of organic material (peat and kerogene).

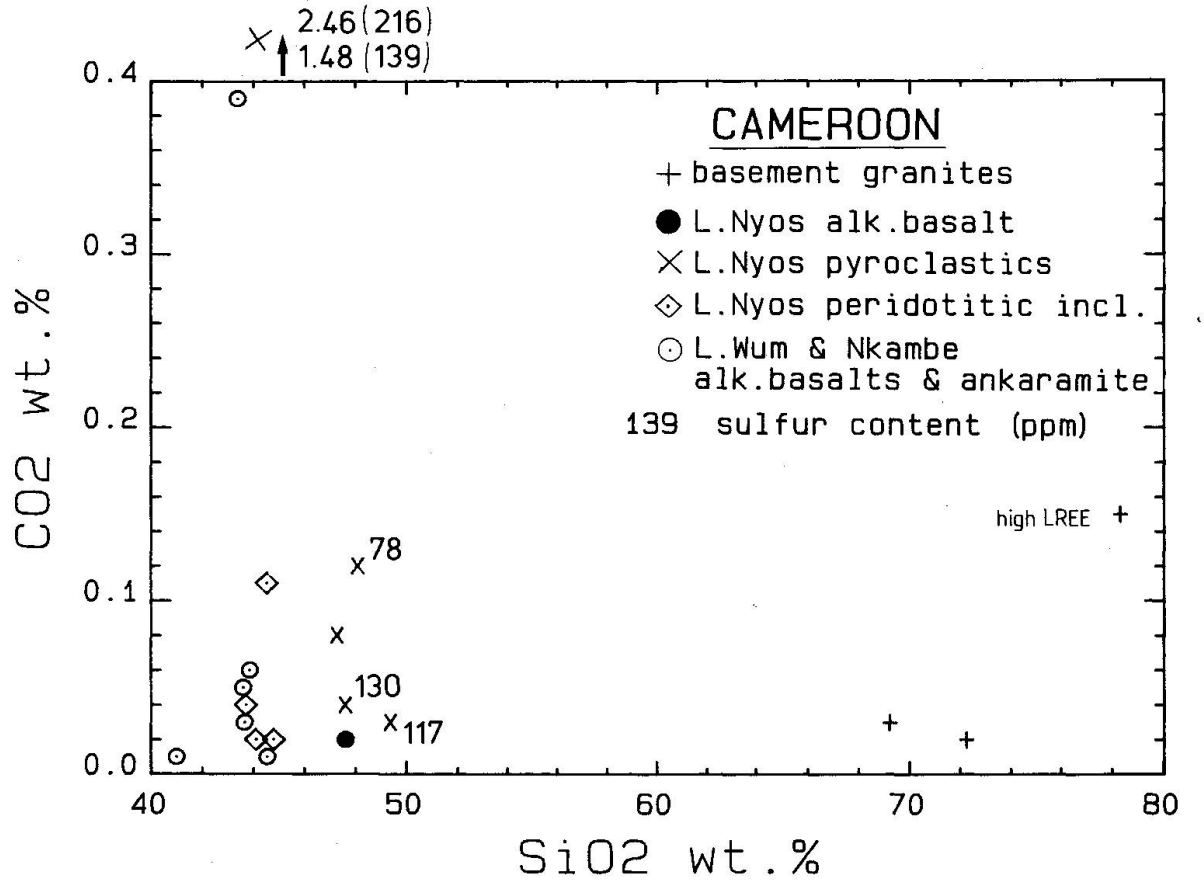

Fig. 13 SiO_2 versus CO_2 from the volcanic rocks, peridotitic nodules and basement rocks from Lake Nyos, Lake Wum and Nkambe.

All alkalic basalts, basanites and ankaramites have high Ba (500–600 ppm), Sr (800–900 ppm) and light rare earth elements (LREE) concentrations. These features are typical in alkalic rock series. However, the very high LREE concentrations in the hydrothermally altered granites from the southern end of Lake Nyos are unusual. We relate this to metasomatic enrichment by hydrothermal processes.

As often pointed out, LREE are strongly hygromagmatophile elements and are trapped in magmatic volatiles and fluids. Such an enrichment can be produced by separation of fluids from a mantle derived melt (WASS and RODGERS, 1980). Often the LREE are closely related with other hygromagmatophile elements such as Rb, Sr and Ba. A significant enrichment of Ba has been recognized in many thermal springs in the volcanic fields along the Cameroon line. This is a further fact to demonstrate the close genetical link between the volcanic activity and mantle derived fluids and volatiles migrating through the crust.

3. Conclusions

3.1. THE ORIGIN OF CARBON DIOXIDE

In NW-Cameroon three areas of magmatic activity can be established: The volcanic fields of Foumbot/Lake Manoun, Bamboui and the region between Lake Wum, Lake Nyos and Nkambe. The magmatic activity is underlined by hydrothermal springs and earthquake activity.

Most of the volcanic rocks produced in these areas are alkalic olivine basalts, ankaramites and basanites, and represent magmas which have been formed in the upper mantle by processes of partial melting and subseqent fractional crystallisation. In many cases, these alkalic lavas carry peridotitic nodules (spinel and pargasite bearing lherzolites and harzburgites) which indicate their mantle origin.

The alkaline magmatism extends over a long distance from the South Atlantic into the West African continent (Cameroon line) and marks a deep seated system of fracture zones. The crystalline Precambrian basement in the active volcanic fields of NW-Cameroon has a strong fault pattern with three major directions N–S, NE–SW, NNE–SSW.

NW-Cameroon is a zone of very high precipitation (> 3 meters/year). During the rainy season, the large fault systems can easily be filled with meteoric water. The maars are the results of phreato-magmatic activity which happens when hot basaltic magma ascends along one fault plane and intersepts another fault filled with cold water. A model of this process is shown in Fig. 14 and 15.

Based on all petrological and chemical data from the maar lakes in NW-Cameroon, the magmatic origin of CO_2 is very plausible. Normally, the gas appears together with the lavas (SATO, 1978; BARNES and MCCOY, 1979; GERLACH, 1980; GERLACH and GRAEBER, 1985; and FUKUTA, 1986) as possible exsolution but also reaches the surface as pre- or post-volcanic exhalations (mofettes) from the vents, indicating a magma reservoir at greater depth.

In addition, isotopic investigations (SIGURDSSON et al., 1986; KUSAKABE et al., 1987; TUTTLE et al., 1987) on the maar waters confirmed the magmatic, mantle derived origin of CO_2. The $\delta^{13}C_{PDP}$ (%) values of both, the total dissolved carbonate and the exsolved CO_2 cluster between -2.0 and -8.0, which overlap exactly the range of values obtained in diamonds and carbonatites (for review, see MATTEY, 1986) and denying the biogenic origin. The $^3He/^4He$ ratios of exsolved gases from the Lake Nyos bottom waters yielded values of 7.1. and 7.2., which are 5 times the atmospheric value and typical for mantle derived gases (SANO et al., 1982; CORNIDES et al., 1986).

For the Lake Nyos case, the gas seems to have reached the surface along a zone of weakness in a post-eruptive ascent from the upper mantle (Fig. 15).

The peridotitic nodules consist of harzburgites and spinel lherzolites which equilibrated under temperatures between 1020 and 950 °C and pressures be-

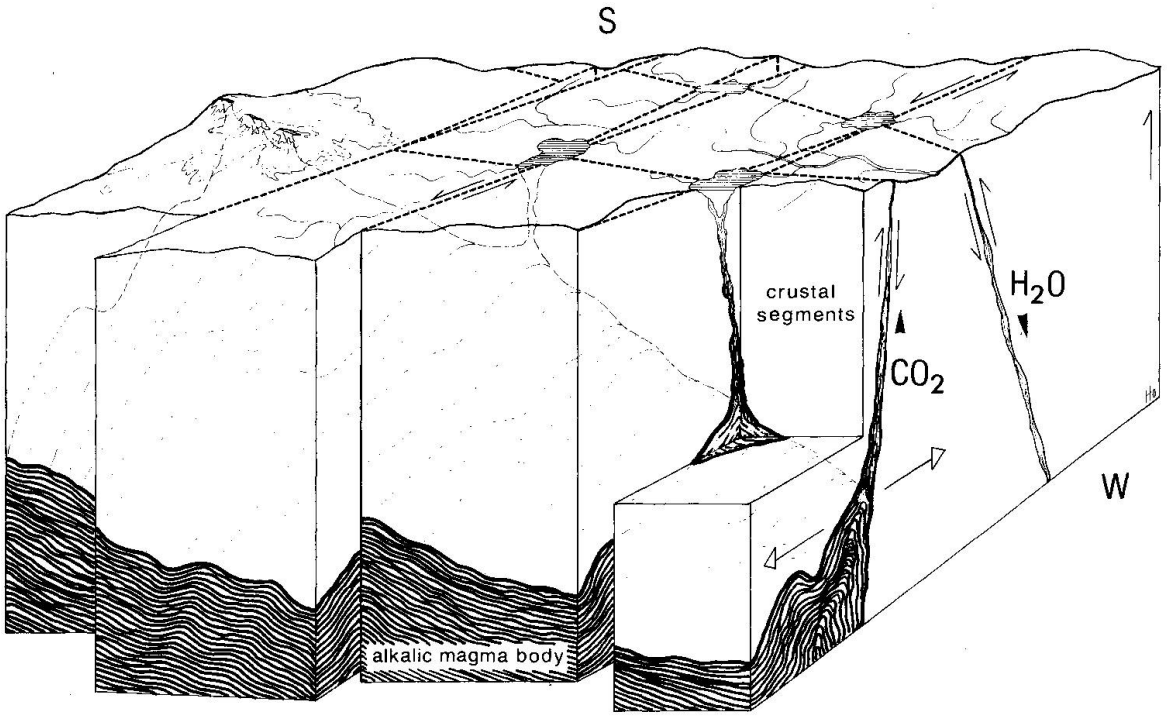

Fig. 14 Model (not to scale) of phreato-magmatic processes which lead to the formation of maars in NW-Cameroon. The intersection of a two-dimensional ascent of magma along a fault plane with a water filled thrust generates phreatomagmatic eruptions forming diatremes and maars. An intersection of magma with a dry fault only produces dikes and scoria cones, as well as fissure eruptions at the surface. The arrows indicate tensional features as well as normal faulting.

tween 18 and 11 kbar (or 50 and 35 km depth respectively). These mantle rocks contain small amounts of pargasitic amphibole, which indicated the presence of water at this depth. However, the total carbon contents are very low in the peridotitic nodules (40–100 ppm). Similar values in amphibole bearing lherzolites from alkalic basalts have been reported by MATHEZ et al. (1984). In contrast, CO_2 in the alkalic basalts and in the ankaramite seem to be enriched (Table 4 and Fig. 13).

The differences of CO_2 contents between the basaltic hostrocks and the mantle xenoliths can be explained by a simple reaction process in the upper mantle (Fig. 16). Under reducing conditions in this environment, where primitive alkalic melts are generated by partial melting from fertile lherzolites, CO_2 is not stable (GOLD and SOTER, 1980). It seems that C occurs as condensed carbonaceous matter (e.g. diamonds) or as CH_4. From the moment water was able to enter this system (probably close to the mantle/crust boundary), CO_2 could be produced by the reaction: $CH_4 + 2\ H_2O \leftrightarrow CO_2 + 4\ H_2$. This reaction proceeds to the left side under increasing pressure and decreasing temperature (FUKUTA, 1986).

It appears that under Lake Nyos the reaction proceeded almost completely to the right. Methane has not been detected in the mud and soil samples of the

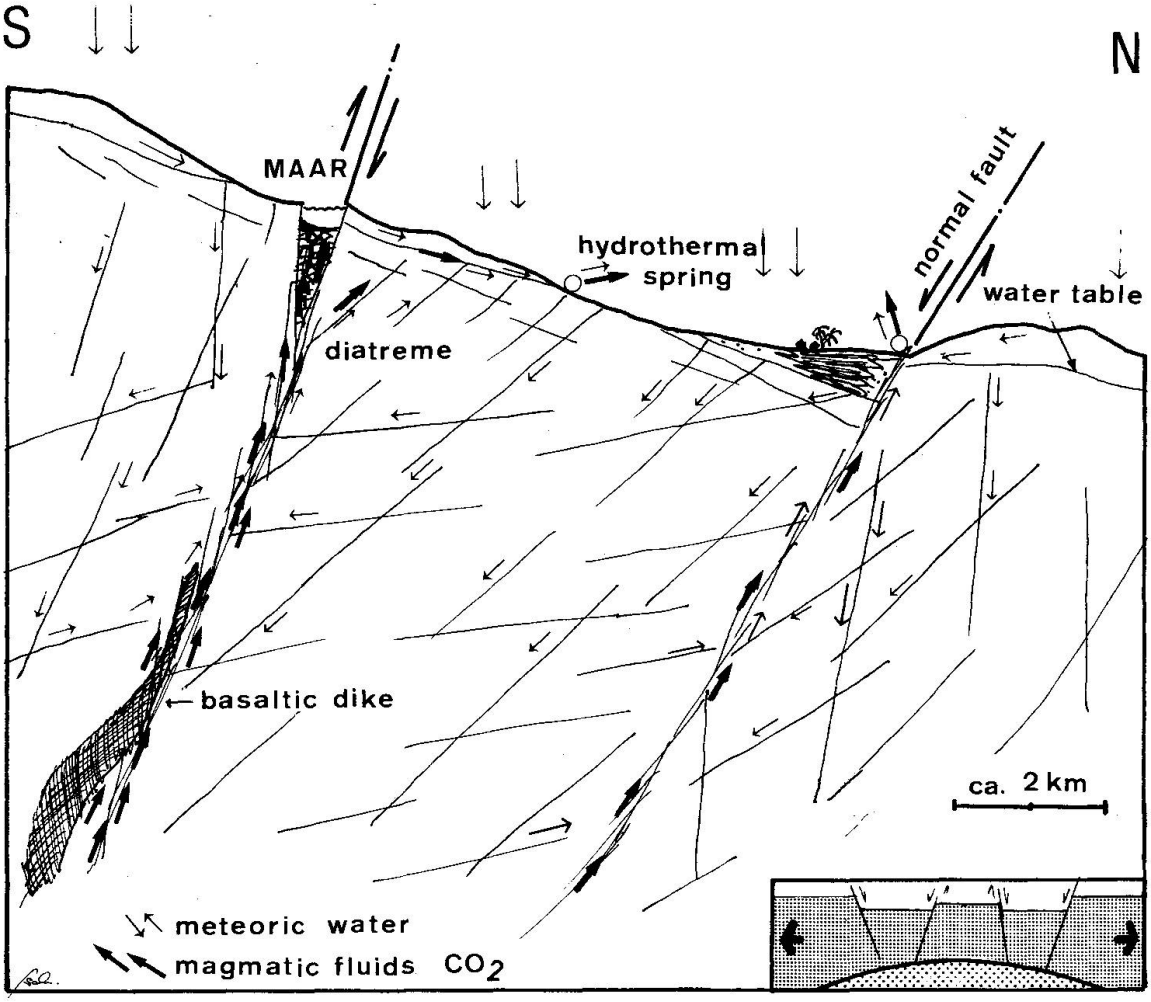

Fig. 15 Hypothetical paths of migration of meteoric water and magmatic fluids and gases in the Lake Nyos area. The hydrothermal water is heated at shallow crustal levels by a high regional geothermal gradient. This figure also shows the possible influx of organic CO_2 from the tropical vegetation into the meteoric water.

lake. It cannot be responsible for the burning effects. Self-ignition of methane in a CO_2 enriched atmosphere seems to be very unlikely.

If the H_2 gas leaves the ascending basaltic magma, f_{O_2} has to increase in the melt (SATO, 1978). H_2 was probably the reason for the small burns on the trees and crops during the gas burst. Further evidence for H_2 in the gas was the observed explosion and a lightning over Lake Nyos on December 30, 1986 (CHEVRIER and LE GUERN, 1987).

Hydrogen sulfide and chlorine in minor concentrations may have accompanied the outburst of CO_2 and H_2 and partly reacted at the surface to H_2SO_4 and HCl causing the observed burns in the lungs and on the skin of the victims.

3.2. THE LETHAL GAS BURST

A maar with its diatreme underneath provide ideal migration paths for hydrothermal fluids (Fig. 15). These fluids are mainly meteoric waters enriched in

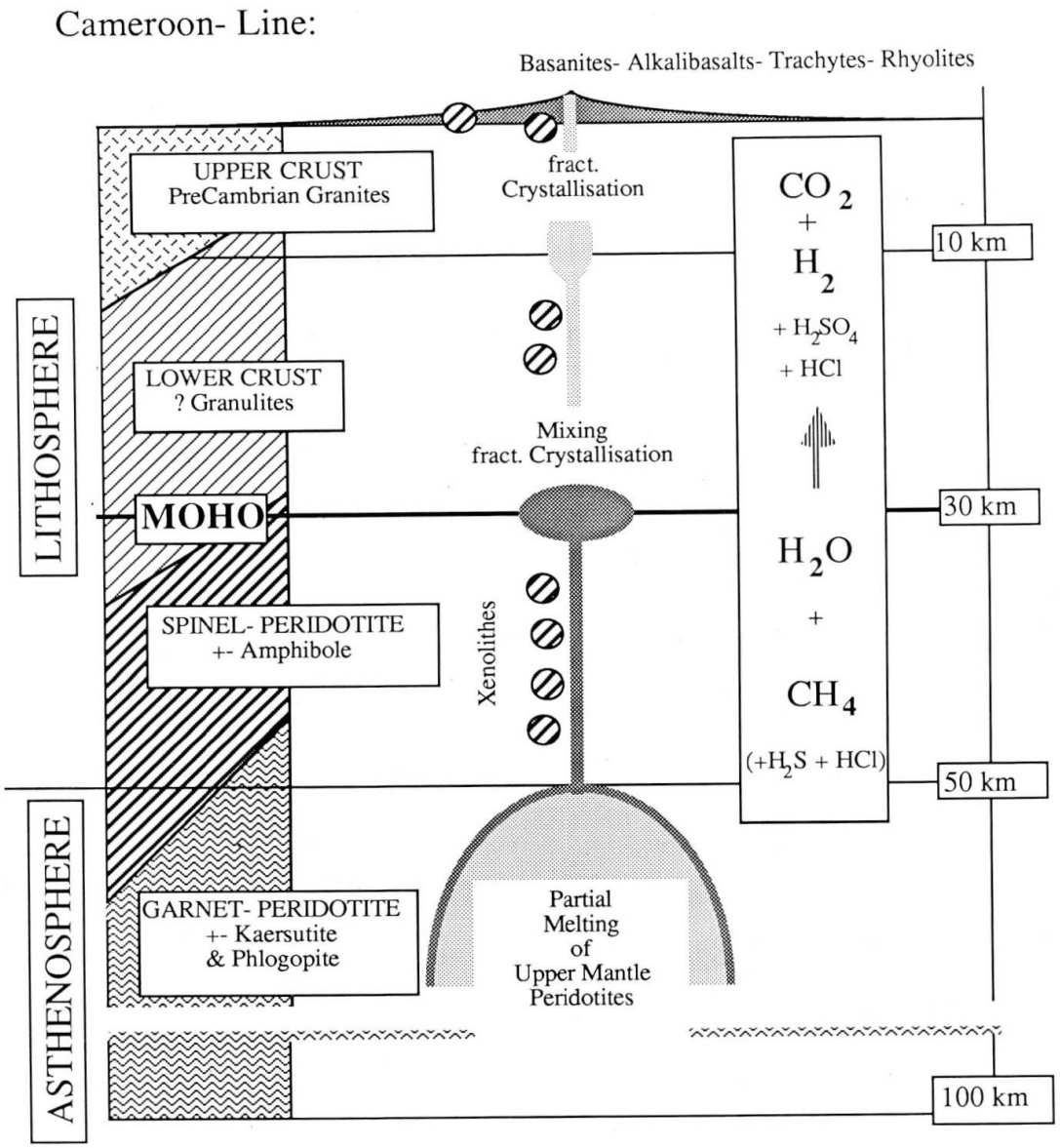

Fig. 16 The magmatic origin of CO_2 in the upper mantle and crust below NW-Cameroon.

mantle derived CO_2 and associated gases. However, the amount and production rate of the ascending CO_2 and accompaning gases are unknown and is dependent on the amount of magmatic activity and influx of water. In addition, the pyroclastic filling of the diatreme and the lake sediments may act as a filter and catalyst for the reactive gases, such as Cl, F, SO_2, etc. The minimum amount of carbon dioxide, which is necessary to form the Lake Nyos lethal gas cloud, is estimated of only 0.15 cubic kilometres.

Two possibilities of gas accumulation and storage can be envisaged:

- The morphological configuration of a maar and its volcanic and epiclastic sediments at the bottom must represent an ideal trap for the gases.

- The other storage capacity is provided by the lake water itself. Limnological investigations of Lake Manoun (SIGURDSSON, 1986) and Lake Nyos (KUSA-

KABE et al., 1987, OSKARSSON, 1987; TIETZE, 1987 and TUTTLE et al., 1987) showed temperature and chemical stratification in the water columns with CO_2 enrichment at the bottoms.

The gas release, finally, may have been caused by several factors depending on the nature of the gas reservoir:

1. If the sediments prevented the migration of gas to the surface, then the gas had to be stored beneath and partially within the caprock. As a consequence, a continuous production of gas raised the internal pressure of the gas deposit. The situation becomes critical when the gas pressure in the reservoir approaches the sum of lithostatic and hydrostatic pressure of the overlying sediments and water column. At this point, several events such as earthquakes, elevated gas inflow, increase of temperature etc., could trigger the leaking of the caprock and generate the outbreak of great volumes of gas within a very short time.

According to the asymmetrical shape of the destroyed area the release of the gases seems to have happened in the continuation of the young fault (Fig. 3 and 4) causing a gas/water bubble which was directed to the south. The water flowed then with great speed directly back into the lake without creating a flood-wave to the north. This phenomenon can be explained by the sinking of the lake floor. The gas was trapped below the lake sediments of the lake and after the outbreak, left a volume deficiency behind.

2. The release of CO_2 from a CO_2 supersaturated water layer could have been triggered by an overturn of the water column, due to nonviolent processes, such as to continuous influx of CO_2, temperature (atmospheric) changes and instability of the equilibria between CO_2, organic carbon, HCO_3^- and ferrous iron (SIGURDSSON et al., 1986; OSKARSSON, 1987) or by discontinous events like earthquake and landslide activity.

In order to evalute the two possible triggering processes an investigation of the uppermost meters of the lake sediments would provide clarifing answers.

The asymmetrical pattern of the mechanical destruction on the southern side of Lake Nyos points to a jetlike outburst of the gas, accompanied with a water bubble which caused the uprooting of the trees. Finally, CO_2 and the other minor amounts of lethal gases with densities greater than air had to flow towards the north down into the deeper parts of the area and dissipating slowly with the air.

3.3. PREVENTION OF FURTHER GAS ERUPTIONS BY DRILLING OPERATIONS

The following procedures have been suggested at the "Internat. Scientific Conference on the Causes of Lake Nyos Disaster", March 1987 at Yaounde, Cameroon:

- In our opinion a gas warning system using gas detectors in a risky area would not be very effective because of the fast and unpredictable nature of the gas bursts. Rapid dissipation of the gases would make it impossible for the residents to bring themselves to safety. In addition, such a warning system seems to be rather inefficient due to communication problems in the sparsely populated hilly region. Most of the inhabitants are the nomadic Fulani which live in a number of scattered camps.

- Because of these reasons we suggest a controlled gas release from possibly trapped gas lenses within or at the base of the lake sediments or from the intersections between the lakes and larger fault zones. In the case of Lake Nyos the gas release can be achieved in two ways:

- by inclined drilling from the outside into the lake sediments and penetrating the southern NW–SE striking fault;
- or by lowering the hydrostatic pressure of the lake by reducing the water level and using an external plumbing system.

- First priority for gas drilling operations should be given to all those maar lakes which are located in the vicinity of larger villages. The young maars (< 1000 years) with steep morphologies and shorelines seem to be more dangerous than the older maars (> 1000 years) with smooth morphologies and eroded tuff rings.

For all cases, and especially for security reasons, we propose inclined drilling to an average depth of 700 m. At this depth, the funnel-shaped maars and diatremes terminate.

- Before drilling a detailed geological investigation (mapping) of the areas is required. The exact position of the drill sites should be determined after consideration of the following factors: the strike and dip of the regional faults, the size and morphology of the maars and the ease of access with mobile drilling equipment including gas blowout preventers.

Appendix

Analytical techniques

Mineral Compositions (Tab. 3 A–F) were determined using an automated ARL SEMQ microprobe equipped with an X-ray energy dispersive analyser (TN 2000 by Tracor Northern). Five crystal X-ray spectrometer and the X-ray energy dispersive system were applied simultaneously for quantitative analyses. An acceleration potential of 15 KV with a sample current of 20 nA (measured on brass) was applied yielding beam size of 0.2 µm. For X-ray energy data collection, integration time including dead-time was 20 seconds resulting in counting statistics better than 1 % (1 sigma) for the minor and major elements. Natural and synthetic oxides and silicates were used as standard materials. The samples as well as the standards were coated with 20 Å of carbon. On-line corrections for drift, dead-time and back-ground were applied to the raw data. Full correction for X-ray fluorescence (by characteristic and continuum excitation) were based on a ZAF program for the CDC Cyber-720 computer system at the ETH Zürich.

Major-element bulk chemical composition (Tables 4 and 5) was determined by the X-ray fluorescence (XRF) analysis of glass beads. The glass beads were fused from ignited powders plus $Li_2B_4O_7$ (⅕ ratio) in a gold-platinum pan at 1150°C (DIETRICH et al., 1976). The XRF analyses were performed with an automatic Philips sequential spectrometer (PW 1450) at the Eidgenössische Materialprüfanstalt, Dübendorf, Switzerland. The data were corrected for drift, background and matrix effects. Twelve USGS rock samples were used for calibration. FeO content was determined colorimetrically. The analysis of CO_2, performed with a Coulomat CS701, was based on coulometric alkalimetric titration (SIXTA, 1977). H_2O+ content was calculated from igneous loss, iron oxidation, and CO_2. Nb, Zr, Y, Sr, U, Rb, Th, Pb, Ga, Zn, Cu, Ni, Co, Cr, V, Ce, Nd, Ba, La, Sc, and S trace-element abundances were analysed by using the synthetic background method, in which major-element contents are known. A computer program was used to calculate background, interference, and mass absorption effects as well as standard deviations (NISBETT et al., 1979). The USGS reference samples were used for calibration. The resulting accuracies were ± 2 to 3% at 1000 ppm, ± 5 to 10% at 100 ppm, and ± 10 to 20% at 10 ppm. A chromium tube was used, and detection limits were around 3–5 ppm for most trace elements.

Tab. 3A Microprobe analyses of olivine.

	Lake Nyos Lherzolitic Nodules				Nkambe Ankaramite		Lake Nyos Alk.Basalt	
Sample	P3 OL4 core	P3 OL5 rim	P4 OL1 rim	P4 OL3 rim	NK OL6 core	NK OL8 rim	LN OL3 core	LN OL1 rim
SiO2	41.33	41.04	40.86	41.19	40.35	38.59	40.28	39.33
FeO	9.17	9.56	8.77	8.70	15.94	20.57	15.96	20.10
MnO	0.16	0.14	0.16	0.13	0.25	0.41	0.29	0.39
MgO	49.74	50.30	49.70	50.27	44.81	41.01	44.21	40.73
NiO	0.32	0.29	0.33	0.34	0.18	0.15	0.28	0.19
CaO	0.09	0.07	0.06	0.05	0.28	0.48	0.21	0.25
Total	100.81	101.39	99.89	100.69	101.82	101.21	101.23	100.99
	CATIONS assuming stoichiometry and charge balance							
Si	1.0023	0.9893	0.9982	0.9975	0.9988	0.9814	1.0046	1.0026
Fe2	0.1859	0.1927	0.1792	0.1763	0.3300	0.4375	0.3329	0.4284
Mn	0.0033	0.0028	0.0032	0.0027	0.0053	0.0087	0.0062	0.0084
Mg	1.7981	1.8077	1.8102	1.8147	1.6536	1.5548	1.6439	1.5477
Ni	0.0063	0.0057	0.0065	0.0066	0.0036	0.0032	0.0057	0.0039
Ca	0.0023	0.0018	0.0017	0.0014	0.0074	0.0130	0.0056	0.0069
	ENDMEMBERS							
Forsterite	0.900	0.898	0.904	0.906	0.824	0.766	0.822	0.773
Fayalite	0.093	0.096	0.089	0.088	0.164	0.215	0.166	0.214

Tab. 3B Microprobe analyses of orthopyroxene from Lake Nyos lherzolitic nodules.

Sample	P3 OPX2 core	P3 OPX1 rim	P4 OPX5 core	P4 OPX6 rim
SiO2	56.71	56.28	55.55	56.01
TiO2	0.09	0.13	0.17	0.13
Cr2O3	0.31	0.29	0.25	0.24
Al2O3	2.36	2.24	4.06	4.24
Fe2O3	0.38	1.09	1.42	0.00
FeO	5.67	4.91	4.63	5.45
MnO	0.16	0.13	0.15	0.13
MgO	34.03	34.21	33.92	33.66
NiO	0.11	0.06	0.09	0.09
CaO	0.61	0.58	0.57	0.59
Na2O	0.11	0.13	0.11	0.10
Total	100.54	100.05	100.92	100.66
CATIONS assuming stoichiometry and charge balance				
Si	1.9446	1.9374	1.8961	1.9131
Ti	0.0024	0.0035	0.0043	0.0034
Cr	0.0083	0.0079	0.0067	0.0066
Al	0.0953	0.0908	0.1633	0.1709
Fe3	0.0099	0.0283	0.0365	0.0000
Fe2	0.1625	0.1412	0.1323	0.1557
Mn	0.0048	0.0038	0.0044	0.0037
Mg	1.7394	1.7554	1.7260	1.7139
Ni	0.0029	0.0016	0.0024	0.0025
Ca	0.0223	0.0213	0.0207	0.0218
Na	0.0076	0.0088	0.0073	0.0066
SITE distribution and RATIOS				
xMg Fe(II+)	0.915	0.926	0.929	0.917
xMg Fe(tot)	0.910	0.912	0.911	0.917
Al(IV)	0.055	0.063	0.104	0.087
Al(VI)	0.040	0.028	0.059	0.084
ENDMEMBERS				
Diopside	0.020	0.020	0.019	0.020
Wollastonite	0.011	0.011	0.010	0.011
Enstatite	0.847	0.851	0.818	0.820
Ferrosilite	0.079	0.068	0.063	0.074
R2R3AlSiO6	0.051	0.056	0.095	0.080

Tab. 3C Microprobe analyses of clinopyroxene.

	Lake Nyos Lherzolitic Nodules				Nkambe Ankaramite			
Sample	P3 CPX5 core	P3 CPX4 rim	P4 CPX5 core	P4 CPX6 rim	NK CPX5 core	NK CPX6 rim	NK CPX3 core	NK CPX4 rim
SiO2	52.50	53.33	53.94	51.76	41.94	47.53	44.33	44.71
TiO2	0.53	0.60	0.57	0.52	5.20	3.08	4.59	3.77
Cr2O3	0.72	0.78	0.60	0.58	0.18	0.00	0.00	0.00
Al2O3	5.61	5.58	7.30	6.78	7.52	6.80	9.27	8.51
Fe2O3	2.25	0.07	0.23	2.40	2.27	3.50	3.22	3.82
FeO	0.57	2.39	2.40	0.43	10.25	3.69	4.00	4.77
MnO	0.09	0.08	0.09	0.11	0.21	0.17	0.13	0.14
MgO	15.23	15.24	15.07	14.84	12.36	13.02	11.46	11.69
NiO	0.05	0.08	0.00	0.05	0.06	0.06	0.04	0.00
CaO	20.49	20.37	20.70	20.70	20.73	23.32	23.34	21.85
Na2O	1.97	1.83	1.97	1.89	0.42	0.56	0.56	0.66
K2O	0.01	0.01	0.02	0.02	0.03	0.02	0.03	0.09
Total	100.02	100.34	102.87	100.07	101.16	101.74	100.99	100.00
	CATIONS assuming stoichiometry and charge balance							
Si	1.8945	1.9176	1.8899	1.8672	1.5966	1.7404	1.6446	1.6759
Ti	0.0144	0.0161	0.0150	0.0141	0.1487	0.0847	0.1281	0.1064
Cr	0.0205	0.0222	0.0166	0.0165	0.0055	0.0000	0.0000	0.0000
Al	0.2384	0.2363	0.3014	0.2882	0.3371	0.2933	0.4053	0.3758
Fe3	0.0611	0.0019	0.0060	0.0651	0.0651	0.0964	Q.0899	0.1076
Fe2	0.0173	0.0718	0.0704	0.0130	0.3262	0.1129	0.1242	0.1493
Mn	0.0026	0.0023	0.0025	0.0033	0.0068	0.0052	0.0041	0.0044
Mg	0.8193	0.8168	0.7873	0.7984	0.7013	0.7107	0.6335	0.6531
Ni	0.0016	0.0022	0.0000	0.0014	0.0017	0.0016	0.0013	0.0000
Ca	0.7922	0.7847	0.7769	0.7999	0.8456	0.9146	0.9278	0.8772
Na	0.1379	0.1278	0.1337	0.1325	0.0309	0.0397	0.0405	0.0481
K	0.0005	0.0005	0.0008	0.0007	0.0016	0.0011	0.0015	0.0042
	SITE distribution and RATIOS							
xMg Fe(II+)	0.979	0.919	0.918	0.984	0.683	0.863	0.836	0.814
xMg Fe(tot)	0.913	0.917	0.912	0.911	0.642	0.772	0.747	0.718
Al(IV)	0.105	0.082	0.110	0.133	0.337	0.260	0.355	0.324
Al(VI)	0.133	0.154	0.191	0.155	0.000	0.034	0.050	0.052
	ENDMEMBERS							
Diopside	0.685	0.659	0.625	0.668	0.447	0.635	0.584	0.537
Wollastonite	0.351	0.359	0.341	0.341	0.329	0.370	0.351	0.332
Enstatite	0.410	0.410	0.394	0.400	0.351	0.356	0.317	0.327
Ferrosilite	0.009	0.036	0.035	0.007	0.163	0.056	0.062	0.075
Pyroxmangite	0.001	0.001	0.001	0.002	0.003	0.003	0.002	0.002
CaAl2SiO6	0.056	0.028	0.063	0.087	0.000	0.034	0.050	0.052
CaFe2SiO6	0.000	0.000	0.000	0.000	0.033	0.056	0.048	0.055
CaCr2SiO6	0.020	0.022	0.017	0.016	0.005	0.000	0.000	0.000
Acmite	0.061	0.002	0.006	0.065	0.033	0.041	0.042	0.052
Jadeite	0.077	0.126	0.128	0.068	0.000	0.000	0.000	0.000
CaTiAl2O6	0.014	0.016	0.015	0.014	0.149	0.085	0.128	0.106

Tab. 3C (Continued).

	Lake Nyos Alkalic Basalt			
Sample	LN CPX1 core	LN CPX2 rim	LN CPX3 core	LN CPX4 rim
SiO2	44.59	43.63	45.72	43.77
TiO2	4.15	4.59	4.08	4.23
Cr2O3	0.18	0.26	0.09	0.08
Al2O3	8.29	9.79	8.50	9.33
Fe2O3	5.16	4.17	3.71	4.74
FeO	4.16	4.81	5.81	4.04
MnO	0.12	0.15	0.14	0.16
MgO	11.89	11.26	11.87	11.49
NiO	0.00	0.04	0.07	0.06
CaO	21.60	21.89	21.94	21.96
Na2O	0.83	0.67	0.66	0.70
K2O	0.09	0.08	0.02	0.04
Total	101.05	101.36	102.60	100.60
Si	1.6575	1.6197	1.6751	1.6337
Ti	0.1161	0.1283	0.1125	0.1188
Cr	0.0052	0.0076	0.0025	0.0024
Al	0.3631	0.4283	0.3668	0.4102
Fe3	0.1442	0.1165	0.1023	0.1331
Fe2	0.1293	0.1494	0.1778	0.1261
Mn	0.0036	0.0049	0.0044	0.0050
Mg	0.6588	0.6234	0.6482	0.6393
Ni	0.0000	0.0013	0.0020	0.0017
Ca	0.8601	0.8707	0.8611	0.8783
Na	0.0598	0.0482	0.0468	0.0507
K	0.0044	0.0038	0.0008	0.0019
xMg Fe(II+)	0.836	0.807	0.785	0.835
xMg Fe(tot)	0.707	0.701	0.698	0.712
Al(IV)	0.342	0.380	0.325	0.366
Al(VI)	0.021	0.048	0.042	0.044
Diopside	0.531	0.499	0.507	0.525
Wollastonite	0.319	0.311	0.325	0.316
Enstatite	0.329	0.312	0.325	0.320
Ferrosilite	0.065	0.075	0.089	0.063
Pyroxmangite	0.002	0.002	0.002	0.002
CaAl2SiO6	0.021	0.048	0.042	0.044
CaFe2SiO6	0.080	0.064	0.055	0.080
CaCr2SiO6	0.005	0.008	0.003	0.002
Acmite	0.064	0.052	0.048	0.053
Jadeite	0.000	0.000	0.000	0.000
CaTiAl2O6	0.116	0.128	0.112	0.119

Tab. 3D Microprobe analyses of pargasite from lherzolitic nodule Lake Nyos.

Sample	P4 AMP1	P4 AMP4	P4 AMP5
SiO2	43.57	42.88	43.44
TiO2	3.27	2.94	3.14
Cr2O3	0.82	0.82	0.83
Al2O3	14.96	15.40	14.43
Fe2O3	3.00	3.78	3.60
FeO	1.15	0.37	0.85
MnO	0.05	0.05	0.06
MgO	16.98	17.20	17.24
NiO	0.12	0.10	0.09
CaO	10.52	10.71	10.67
Na2O	4.04	4.10	3.98
K2O	0.05	0.04	0.05
H2O	2.14	2.14	2.14
Total	100.69	100.54	100.51
CATIONS calculated on the basis of 13. cations and 24. oxygens			
Si	6.0921	6.0058	6.0913
Ti	0.3443	0.3101	0.3309,
Cr	0.0910	0.0903	0.0921
Al	2.4644	2.5428	2.3853
Fe3	0.3152	0.3981	0.3796
Fe2	0.1349	0.0439	0.0995
Mn	0.0065	0.0057	0.0073
Mg	3.5381	3.5921	3.6040
Ni	0.0136	0.0113	0.0099
Ca	1.5760	1.6076	1.6037
Na	1.0964	1.1141	1.0824
K	0.0084	0.0078	0.0087
OH	2.0000	2.0000	2.0000
SITE distribution and RATIOS			
xMg (FeII+)	0.963	0.988	0.973
xMg (Fe tot)	0.887	0.890	0.883
Al(IV)	1.908	1.994	1.909
Al(VI)	0.556	0.549	0.477
Na (M4)	0.424	0.392	0.396
Na (A)	0.672	0.722	0.686

Tab. 3E Microprobe analyses of chromespinel, ulvoespinel and ilmenite.

	Chromespinel in Lherzolitic Nodules				Nkambe Cr-Spinel in Olivine		
Sample	P3 SPI4 rim	P3 SPI5 core	P4 SPI5 core	P4 SPI6 rim	NK SPI8	NK SPI6	NK SPI5
TiO2	0.08	0.12	0.05	0.07	2.92	1.81	3.23
Cr2O3	10.65	10.64	8.11	7.96	14.80	11.80	14.30
Al2O3	56.46	56.85	59.89	59.85	37.75	44.67	34.42
Fe2O3	3.96	3.22	1.64	1.76	12.28	10.39	15.77
FeO	7.36	7.76	8.53	8.11	17.78	14.37	17.36
MnO	0.10	0.09	0.09	0.11	0.24	0.19	0.26
MgO	21.84	21.60	21.25	21.44	14.52	16.81	14.44
NiO	0.37	0.39	0.33	0.40	0.30	0.36	0.33
CaO	0.00	0.02	0.00	0.02	0.07	0.04	0.09
Total	100.82	100.67	99.90	99.70	100.67	100.45	100.20
	CATIONS assuming stoichiometry and charge balance						
Ti	0.0016	0.0022	0.0011	0.0013	0.0630	0.0375	0.0709
Cr	0.2156	0.2156	0.1638	0.1608	0.3354	0.2574	0.3297
Al	1.7048	1.7179	1.8030	1.8028	1.2748	1.4523	1.1836
Fe3	0.0764	0.0620	0.0314	0.0339	0.2647	0.2158	0.3462
Fe2	0.1577	0.1663	0.1823	0.1734	0.4260	0.3314	0.4234
Mn	0.0022	0.0020	0.0020	0.0024	0.0058	0.0046	0.0065
Mg	0.8340	0.8255	0.8093	0.8169	0.6204	0.6915	0.6280
Ni	0.0077	0.0080	0.0067	0.0082	0.0069	0.0080	0.0077
Ca	0.0000	0.0004	0.0000	0.0004	0.0023	0.0012	0.0027
	SITE distribution and RATIOS						
xMg Spinel	0.831	0.822	0.808	0.815	0.551	0.644	0.551
xFe(II+) Spi	0.157	0.166	0.182	0.173	0.379	0.308	0.371
yAl Spinel	0.854	0.861	0.902	0.903	0.680	0.754	0.637
yCr Spinel	0.108	0.108	0.082	0.080	0.179	0.134	0.177
yFe (III+)	0.038	0.031	0.016	0.017	0.141	0.112	0.186
	ENDMEMBERS						
Magnetite	0.006	0.005	0.003	0.003	0.043	0.029	0.053
Mg-Ferrite	0.032	0.026	0.013	0.014	0.088	0.078	0.118
Spinel	0.717	0.717	0.736	0.744	0.426	0.527	0.405
Hercynite	0.133	0.140	0.164	0.155	0.206	0.195	0.182
Chromite	0.017	0.018	0.015	0.014	0.055	0.035	0.051
Mg-Cromite	0.091	0.090	0.067	0.066	0.113	0.094	0.114
Ulvoespinel	0.002	0.002	0.001	0.001	0.063	0.037	0.071

Tab. 3E (Continued).

	Nkambe Spinel matrix sp.	ulvospinel matrix		Lake Nyos sp.in ol		matrix ilmenite		
Sample	NK SPI3	NK USP2	NK USP3	LN SPI1	LN SPI3	LN USP4	LN ILM1	
TiO2	18.30	23.96	24.74	6.99	7.38	20.17	49.13	
Cr2O3	4.14	1.01	0.24	17.96	16.94	2.13	0.26	
Al2O3	9.56	5.49	4.16	16.46	14.86	3.40	0.00	
Fe2O3	22.81	14.66	17.18	21.68	23.61	26.21	8.56	
FeO	37.53	49.63	49.84	24.89	25.94	41.67	33.90	
MnO	0.53	0.74	0.82	0.39	0.41	0.59	0.59	
MgO	7.39	2.72	2.14	9.27	8.63	5.00	5.55	
NiO	0.34	0.00	0.06	0.37	0.39	0.07	0.00	
CaO	0.11	0.26	0.47	0.09	0.09	0.12	0.60	
Total	100.70	99.32	98.81	98.09	98.24	99.36	98.59	
	CATIONS assuming stoichiometry and charge balance							
Ti	0.4651	0.6449	0.6741	0.1742	0.1859	0.5444	0.8937	
Cr	0.1106	0.0286	0.0068	0.4702	0.4484	0.0603	0.0050	
Al	0.3809	0.2314	0.1779	0.6426	0.5864	0.1439	0.0000	
Fe3	0.5801	0.3948	0.4685	0.5404	0.5950	0.7078	0.1558	
Fe2	1.0608	1.4853	1.5104	0.6894	0.7266	1.2505	0.6857	
Mn	0.0152	0.0223	0.0251	0.0110	0.0115	0.0180	0.0121	
Mg	0.3725	0.1453	0.1158	0.4578	0.4307	0.2675	0.2002	
Ni	0.0092	0.0000	0.0018	0.0098	0.0106	0.0021	0.0000	
Ca	0.0038	0.0100	0.0184	0.0031	0.0033	0.0046	0.0156	
	SITE distribution and RATIOS							
xMg Spinel	0.193	0.063	0.049	0.340	0.314	0.128	0.219	xMg romb.Ox
xFe(II+) Spi	0.550	0.642	0.644	0.512	0.530	0.599	0.750	xFe romb.Ox
yAl Spinel	0.355	0.353	0.272	0.389	0.360	0.158		
yCr Spinel	0.103	0.044	0.010	0.284	0.275	0.066		
yFe (III+)	0.541	0.603	0.717	0.327	0.365	0.776		
ENDMEMBERS	ENDMEMBERS							
Magnetite	0.073	0.109	0.125	0.113	0.132	0.128	0.080	Hematite
Mg-Ferrite	0.208	0.081	0.089	0.152	0.160	0.211	0.682	Ilmenite
Spinel	0.137	0.048	0.034	0.181	0.158	0.043	0.012	Mn-Ilmenite
Hercynite	0.048	0.064	0.048	0.135	0.130	0.026		
Chromite	0.014	0.008	0.002	0.100	0.101	0.011		
Mg-Cromite	0.041	0.006	0.001	0.135	0.123	0.019		
Ulvoespinel	0.465	0.645	0.674	0.174	0.186	0.544		

Tab. 3F Microprobe analyses of plagioclase, anorthoclase and alkali feldspar.

	Nkambe Ankaramite								Lake Nyos Alkalic Basalt			
	microphenocrysts			anorthoclase matrix			k-feldspar matrix		microphenocrysts		anorthoclase matrix	
Sample	NK PL1	NK PLG6	NK PL3	NK AN01	NK AN02	NK AN05	NK KFP1	NK KFP3	LN PLG3	LN PLG2	LN AN02	LN AN05
SiO2	50.06	52.16	53.45	52.20	51.01	51.78	62.44	63.47	53.68	53.67	62.51	61.74
TiO2	0.22	0.23	0.15	0.15	0.09	0.10	0.22	0.18	0.20	0.21	0.40	0.76
Al2O3	31.86	30.73	29.31	29.29	31.45	29.31	21.74	20.99	28.72	28.34	22.71	22.42
Fe2O3	0.81	0.37	0.00	1.29	0.91	0.68	0.00	0.00	1.00	0.75	0.90	1.18
MgO	0.06	0.00	0.05	0.47	0.00	0.05	0.00	0.00	0.09	0.06	0.00	0.11
CaO	14.80	13.09	12.01	2.83	0.85	1.72	1.00	1.73	11.97	11.57	4.29	4.37
Na2O	3.15	3.74	4.17	11.23	13.29	12.14	3.42	4.05	4.59	4.88	6.82	7.30
K2O	0.22	0.57	0.56	2.91	3.28	4.41	9.71	9.28	0.43	0.46	3.15	2.83
Total	101.18	100.89	99.70	100.37	100.88	100.21	98.57	99.69	100.67	99.94	100.79	100.72
	CATIONS assuming stoichiometry and charge balance											
Si	2.2609	2.3498	2.4332	2.2297	2.1311	2.1939	2.8815	2.8883	2.4217	2.4327	2.7877	2.7505
Ti	0.0075	0.0079	0.0052	0.0049	0.0029	0.0032	0.0076	0.0060	0.0068	0.0073	0.0135	0.0254
Al	1.6960	1.6312	1.5723	1.4747	1.5487	1.4635	1.1822	1.1255	1.5270	1.5136	1.1933	1.1772
Fe3	0.0275	0.0200	0.0000	0.0416	0.0285	0.0218	0.0000	0.0000	0.0340	0.0257	0.0303	0.0396
Mg	0.0039	0.0000	0.0037	0.0298	0.0000	0.0034	0.0000	0.0000	0.0059	0.0037	0.0000	0.0071
Ca	0.7159	0.6318	0.5858	0.1294	0.0379	0.0782	0.0496	0.0844	0.5787	0.5619	0.2048	0.2088
Na	0.2758	0.3265	0.3676	0.9298	1.0760	0.9975	0.3060	0.3573	0.4013	0.4284	0.5899	0.6305
K	0.0126	0.0328	0.0323	0.1584	0.1749	0.2386	0.5716	0.5384	0.0246	0.0267	0.1794	0.1609
	ENDMEMBERS											
Albite	0.275	0.329	0.373	0.764	0.835	0.759	0.330	0.365	0.399	0.421	0.606	0.630
Anorthite	0.713	0.637	0.594	0.106	0.029	0.060	0.053	0.086	0.576	0.552	0.210	0.209
Orthoclase	0.013	0.033	0.033	0.130	0.136	0.182	0.617	0.549	0.025	0.026	0.184	0.161

Tab. 4 Major and trace element abundances from lavas, pyroclastics and granites from the Lake Nyos - Lake Wum - Nkambe region.

	Lake Nyos						Lake Wum	Nkambe
	basalt	basalt. clasts		soil	granites		basalt	ankaramite
Sample Nr.	LN6	LN7A	LN7F	LN4	LN1	LN3	LW5A	NK2
SiO2 wt.%	47.62	48.08	47.27	45.41	68.80	78.31	43.58	40.98
TiO2	2.61	2.47	2.76	2.15	0.48	0.25	3.17	3.50
Al2O3	15.07	15.41	15.63	16.02	15.90	11.68	15.63	12.96
Fe2O3 tot.	11.87	11.18	11.85	9.84	2.85	3.58	13.35	13.30
MnO	0.17	0.15	0.16	0.15	0.03	<0.01	0.19	0.18
MgO	7.35	8.22	6.58	7.13	0.40	0.27	7.45	10.90
CaO	8.21	7.91	7.92	5.18	1.62	0.27	8.42	11.70
Na2O	3.87	2.58	3.70	1.83	4.31	<0.05	1.99	2.09
K2O	1.81	1.38	1.95	1.54	5.02	1.60	1.70	1.43
P2O5	0.75	0.66	0.72	0.54	0.16	0.13	0.87	0.60
H2O+	0.02	0.96	0.46	6.83	0.32	3.65	2.19	0.86
CO2	0.02	0.12	0.08	2.46 *	0.03	0.15	0.05	0.01
Total	99.37	99.12	99.08	99.08	99.92	99.94	98.59	98.51
Ba ppm:	559	677	563	516	1034	335	648	500
Rb	34	24	41	46	187	96	27	32
Sr	835	829	830	416	291	49	876	920
Pb	<6	<6	<6	<6	20	12	<6	<6
Th	<5	<5	<5	<5	18	6	<5	<5
U	1	<1	1	<1	5	3	<1	1
Nb	51	46	55	46	22	11	63	44
La	71	103	94	116	130	557	122	78
Ce	61	89	85	97	160	170	88	65
Nd	31	46	41	48	57	319	49	40
Y	26	26	28	25	22	71	30	25
Zr	256	265	277	254	252	164	275	179
V	211	309	255	262	65	27	313	330
Cr	201	255	154	275	<10	14	180	351
Ni	135	203	106	223	<3	<3	140	190
Co	67	87	84	57	15	14	70	79
Cu	22	33	43	29	<4	<4	30	46
Zn	99	96	105	77	49	20	111	86
Ga	17	18	18	18	23	13	19	16
Sc	17	23	20	21	5	3	25	26
S	<20	78	<20	216	<20	<20	<20	<20

* CO2 (calculated from total carbon, which was analysed with coulomat under pure oxygene atmosphere).

LN6 : Alkalic basaltic lava from the southern shore of lake Nyos (Fig. 7).

LN7A + 7B : Black, glass rich alkalic basaltic clasts (Fig. 6) containing numerous fragments of granites, gneisses and peridotites.

LN4 : Pyroclastic soil from the SW-delta after the gas outburst.

LN1 : Rapakivi-type granite from the western shore of lake Nyos.

LN3 : Hydrothermally altered granite at southern end of lake Nyos.

LW5A : Alkalic basaltic lava flow from southern shore of lake Wum, containing only few granitic fragments (<0.01 vol.%).

NK2 : Ankaramite from lava flow on Ringroad, ca. 30 km west of Nkambe (Fig. 8).

Tab. 5 Major and trace element abundances from peridotitic inclusions in the Lake Nyos alkali-basaltic pyroclastics.

	harzburgite	spinel (hornblende) lherzolithe	
Sample Nr.	LNP1	LNP3	LNP4
SiO2 wt.%	43.69	44.79	44.09
TiO2	0.03	0.11	0.18
Al2O3	1.47	3.31	3.95
Fe2O3	3.25	3.55	3.56
FeO	5.00	4.50	4.55
MnO	0.13	0.12	0.14
MgO	44.41	40.11	39.59
CaO	1.15	2.77	3.22
Na2O	0.13	0.13	0.20
K2O	<0.01	<0.01	<0.01
P2O5	0.04	0.04	0.04
CO2	0.04	0.02	0.02
Total	99.26	99.45	99.54
V ppm:	43	66	70
Cr	2327	2723	2444
Ni	2293	1913	1827
Co	132	122	117
Zn	50	42	42
Sc	11	15	14

Ultramafic Norm in Oxide % (LENSCH, 1968)			
Cpx Wol	2.12	5.23	6.10
Cpx En1	2.02	5.01	5.85
Cpx Fs1	0.10	0.22	0.26
Opx En2	24.37	32.69	28.21
Opx Fs2	1.20	1.42	1.25
Jad	0.91	0.90	1.40
Olv Fos	61.13	44.63	46.29
Olv Fay	3.01	1.94	2.05
Apt	0.09	0.09	0.09
Spl	1.78	3.56	3.54
Crm	0.29	0.36	0.33
Mgt	2.94	3.20	3.21
Ilm	0.04	0.15	0.24
Total	100.00	100.00	100.00

Tab. 6 Analyses of surface water samples, eight days after the Lake Nyos gas burst.

	Lake Nyos	Lake Wum
pH	6.1	5.7
Conductivity (γ-Siemens)	216	75
CO_2	50	45
SO_2	20	< d.l.
Cl	15	20
Ca	55	< d.l.
Fe	0.3	0.15
SiO_2	23	9

Analytical methods: pH and conductivity with electrical sensors: CO_2, SO_2, Cl; Ca and Fe with titration methods: SiO_2 by absorption spectrometry.
All values in mg/l.
< d.l.: below detection limit.

Tab. 7 Geothermometry and geobarometry.

Method	Reference	Spinel-Lherzolite Nodules Lake Nyos P 3	P 4
Olivine ‖ Spinel	FABRIES (1979)	1150 +– 100 (6)	920 +– 60 (6)
	ENGI (1983)	1100 +– 100 (6)	900 +– 30 (6)
Cpx ‖ Opx	WOOD and BANNO (1973)	1040 +– 25 (25)	1030 +– 20 (9)
	WELLS (1977)	940 +– 20 (25)	920 +– 20 (9)
	HERZBERG (1978)	970 +– 10 (25)	950 +– 20 (9)
	HERVIG and SMITH	1010 +– 20 (25)	940 +– 30 (9)
single Cpx	MERCIER (1976)	990 +– 40 (10) Pressure: 16–18 kbar	940 +– 40 (3) 10–12.5 kbar
single Opx	MERCIER (1976)	990 +– 10 (15) (Pressure: 23–26 kbar	990 +– 10 (3) 18–18.5 kbar)
	SACHTLEBEN and SECK (1981)	970 +– 10 (15)	960 +– 10 (3)
Average and range:		1020°C (940–1150)	950°C (900–1030)

Average temperatures +– statistical standard deviation are given indegrees centigrade ; the numbers in parentheses are the amounts of mineral pairs measured and used for calibrations.

Gas measurements

For the protection of the remaining population and of the Swiss team in the devastated area, oxygen and the concentrations of hydrogene sulfide and carbon monoxide were continually measured by independent electrical detectors. During the measuring period, the values for oxygen never dropped under, nor were the values for H_2S and CO_2 ever over the alarm levels. The gas chromatographs of the GEMAG AG could not be used during the Cameroon mission because of the lack of independent electrical power. At the time, a battery-operated gas chromatograph was not available in Switzerland. All analyses were performed with test-tubes. With this method, a specific amount of air is pumped through a gas indicator. The volume of the colored indicator substance reacts proportionally to the concentration of the tested gas in the air sample. CO_2, CO, SO_2, HCl, H_2SO_4, CH_4, and H_2S were measured. Only the values for CO_2 and SO_2 showed variations different to the normal air composition near the ground.

Carbon dioxide: In the devastated area the concentration of CO_2 was determined in the order of 0.05 vol.% (normal air 0.03 vol.%). These values layed just slightly over the sensibility level of the testing method and therefore only showed a slight increase. An analysis of the ground air from approximately one meter above the shoreline of Lake Wum gave 2.1 vol.% CO_2. Due to lack of time it was impossible to test the regional background concentration of CO_2 in the ground air. The CO_2 contents in ground air gas samples can vary drastically depending on the nature and composition of the soil and underlaying rocks, e.g. in several carbonate-rich environments in Europe the CO_2 contents reach 10 to 20 vol.%. Because the samples taken at Lake Wum are from a carbonate free terraine, and therefore an oxidation of organic material can be rejected, it is possible that the slightly raised values of 2.1 vol.% for CO_2 could be a sign of a gas of volcanic origin.

Sulfur dioxide: The values for SO_2 in the region between Lake Wum and Lake Nyos area varied between 7 and 10 vpm (volumes per million). For comparison, outside the stricken area in the cities of Duala and Bamenda test samples with concentrations of 3–6 vpm SO_2 were measured. These measurements could be influenced from contamination by gasoline and diesel emissions. In Nkambe, a small town without much traffic, no SO_2 was measureable in the air. In addition, these low values have high analytical errors and thus, should only be regarded as qualitative values.

Geothermometry and geobarometry in the Lake Nyos alkalic basalts, peridotitic nodules and the Nkambe ankaramite.

Spinel-olivine: This geothermometer was used to calculate the reequilibration temperature in the partly resorbed olivine phenocrysts (Fig. 8 and Table 3A) which contain small inclusions of chromium-spinel (Table 3E) from the Nkambe ankaramite. These temperatures (Table 7) should give an indication of the cooling behavior of the ankaramitic melt during its uprise in the crust and extrusion. Depending on the range of compositions in the olivines and spinels, a range of temperatures between 1190 and 910 °C (assuming 1 kbar pressure) were derived by using the calibrations of ROEDER et al. (1979) and ENGI (1983). This indicates that the primitive ankaramitic melts started with temperatures at 1200 °C and rapidly cooled reaching the surface. The low temperatures are interpreted as subsolidus temperatures. The still perfect shape of the olivine phenocrysts indicate that the uprise of the melt through the crust must have occurred rather fast.

The use of the spinel-olivine geothermometer in the peridotitic nodules from Lake Nyos also yielded geologically reasonable temperatures (Table 7) assuming a pressure of 15 kbar. The spinel lherzolites P3 gave temperatures between 1000 and 1250 °C, the sample P4 lower temperatures of between 900 and 980 °C.

Clinopyroxene-orthopyroxene: Three different kinds of two-pyroxene geothermometers are currently in use: 1) the solvus geothermometer which is based on the calibration of the enstatite solid solution in diopside (WOOD and BANNO (1973), WELLS (1977), HERZBERG (1978), and others, 2) the Mg–Fe partioning between Cpx and Opx (KRETZ, 1982) and, 3) the Na-partioning between Cpx and Opx (HERVIG and SMITH, 1980). The temperatures obtained with the method of Kretz scattered randomly between 300 and 1200 °C probably due to oxidation processes in the peridotitic nodules from Lake Nyos during the phreatomagmatic eruption. All other temperatures (Table 7) varied between 940 and 1065 °C for the spinel lherzolite P3 and between 900 and 1050 °C for the sample P4 and are consistent with the spinel-olivine geothermometer.

Single clinopyroxene geothermometer and geobarometer: This geothermometer (MERCIER, 1976) is based on the calibration of the diopside component in the system diopside-entstatite. The pressures can also be calculated from single clinopyroxene composition using the combined wollastonite-enstatite and Ca-Tschermaks solid solutions in clinopyroxene. The temperatures obtained (Table 7) are consistent with those derived with the other methods, the pressures for the peridotitic nodules range between 10 and 18 kbar.

Single orthopyroxene geothermometer and geobarometer: Similar temperature and pressure calculations can be performed with orthopyroxene compositions using calibrations from MERCIER (1976) and SACHTLEBEN and SECK (1981). Both methods are calibrated on the pure diopside-enstatite join and can only be used for Fe-poor orthopyroxenes. The temperatures for the sample P3 seem to be a little bit lower than those obtained with the other methods. The pressures are consistently higher than those using the clinopyroxene method by the average 7 kbar. The reason might be due to the calibration of this thermometer.

Fe–Ti-Oxide geothermometry in the Lake Nyos alkalic olivine basalt: The temperature of the last equilibrium (crystallisation of basaltic groundmass) between the cubic (ulvoespinel-magnetite) and the rhombohedral iron-titanium oxide phases (ilmenite-hematite) as well as the oxygene fugacities

have been calculated from the small portions of alkali-basaltic lava (LN6) from Lake Nyos by using the algorithms of GHIORSO and CARMICHAEL (1981).

Three groups of temperatures resulted from these calculations: 1) 1045 °C and with $-\log f_{O_2}$ = 10.1, 2) 1010 °C and $-\log f_{O_2}$ = 10.6 and, 3) 995 °C and $-\log f_{O_2}$ = 10.8. The higher temperatures seem to be very reasonable for rapid cooling processes of a alkali-basaltic lava within a diatreme. The lower values represent subsolidus temperatures of equilibrium.

Summary: The temperatures and pressures obtained from mineral chemistry in the Lake Nyos peridotitic nodules are regarded as PT-conditions in the upper mantle under which these minerals were equilibrated. The spinel lherzolite P3 yields slightly higher temperatures (average of 1020 °C) and higher pressures (average 17 kbar) than the spinel lherzolite P4 (temperatures average 950 °C and pressures average 11 kbar).

Acknowledgements

The authors wish to thank the Minister of territorial administration Jean-Marcel Mengueme, the Governor of the NW-district Joseph Tigie and Brig. General James Tataw for local advice and assistance. Eduard Blaser, Delegate of the Swiss Federal Council for Disaster Relief, expedited our efforts with distinction.

The XRF analyses were made with the assistance of A. Esenwein (EMPA), Dübendorf, Switzerland. J. Horal was responsable for some of the figure drawings and H. Heldstab («Blick»-Magazine) provided some photographs.

Thanks are also due to P. Ulmer, who performed the electron microprobe analyses and to Mrs. Lisa Dietrich, who translated, typed and edited the manuscript. We also thank K. Kelts (EAWAG) Dübendorf, D. Vuichard and M. Engi (Berne) for discussions; V. Lorenz (Mainz) for a most constructive review; W. Hinze from the GEMAG AG and W. Strub (SKH/SDR, Berne) for field assistance and generous support.

This work was financially supported by the Swiss Disaster Relief Unit (Schweizerisches Katastrophenhilfekorps Bern).

References

BARNES, I. and MCCOY, G.A. (1979): Possible role of mantle derived CO_2 in causing two phreatic explosions in Alaska. Geology, Vol. 7, 434–435.

BURKE, K. and DEWEY, J.F. (1973): Plume-generated triple junctions: Key indications in applying plate tectonics to old rocks. J. Geol., 81, 406–433.

CANTAGREL, J.-M., JAMOND, C. and LASSERRE, M. (1978): Le magmatism alkalin de la ligne du Cameroun au Tertiaire inférieur: données géochronologiques K–Ar. C.R. Somm. Soc. Géol. France, 6, 300–303.

CHEVRIER, R.M. and LE GUERN (1987): Etudes comparatives des eaux des lacs Nyos et Wum. Conf. Intern. sur la Catastrophe du Lac Nyos, Yaounde, Cameroun, 16–20 March, 1987, Abstract.

CHAIGNEAU, M., HEKINIAN, R. and CHEMINEE, J.L. (1980): Magmatic gases extracted and analysed from ocean floor volcanics. Bull. Volcanol., Vol. 43/1, 241–253.

CORNIDES, I., TAKAOKA, N., NAGAO, K. and MATSUO, S. (1986): Contribution of mantle-derived gases to subsurfaces gases in a tectonically quiescent area, the Carpathian Basin, Hungary revealed by noble gas measurements. Geochem. Journ. 20, 119–125.

DEUSER, W.G., DEGENS, E.T. and HARVEY, G.R. (1973): Methane in Lake Kivu – new data bearing on its origin. Science, Vol. 81, 51–53.

DIETRICH, V.J., CARMAN, M.F., WYTTENBACH, A. and MCKEE, E.H. (1984): Geochemistry of basalts form Holes 519A, 520, 522B and 524. Deep Sea Drilling Project Leg 73 (South Atlantic). Init. Rep. DSDP, Vol. 7, 579-601

DIETRICH, V.J. and CARMAN, M.F. (in prep.): The petrogenesis of alkalic rocks from the Walvis ridge (South Atlantic): A hot-spot line of alkaline volcanoes.

DIETRICH, V.J., OBERHÄNSLI, R. and WALPEN, P. (1976): Röntgenfluoreszenzanalyse der Silikatgesteine (internal report). Inst. Krist. Petr. ETH, Zürich.

ENGI, M. (1983): Equilibria involving Al-Cr spinel: Mg-Fe exchange with olivine. Experiments, thermodynamic analysis, and consequences for geothermometry. Am. J. Sci. 283A (Orville Volume), 29-71.

FABRIES, J. (1979): Spinel-olivine geothermometer in peridotites from ultramafic complexes. Contrib. Mineral. Petrol. 69, 329-336.

FITTON, J.G. (1980): The Benue trough and Cameroon line—a migrating rift system in West Africa. Earth Planet. Sci. Lett. 51, 132-138.

FITTON, J.G. (1983): Active versus passive continental rifting: evidence from the West African rift system. Tectonophysics 94, 473-481.

FITTON, J.G. and DUNLOP, H.M. (1985): The Cameroon line, West Africa, and its bearing on the origin of oceanic and continental alkali basalt. Earth Planet. Sci. Lett. 72, 23-38.

FITTON, J.G., KILBURN, C.R.J., THIRLWALL, M.F. and HUGHES, D.J. (1983): 1982 eruption of Mount Cameroon, West Africa. Nature, Vol. 306, 327-332.

FUKUTA, O. (1986): Natural gas expected in the lakes originating in the rift valley system of East Africa, and analogous gas in Japan. Amer. Ass. Petrol. Geol., Mem. 40, 445-456.

GERLACH, T.M. (1980): Chemical characteristics of the volcanic gases from Nyiragongo lava lake and the generation of CH_4-rich fluid inclusions in alkaline rocks. J. Volcanol. Geotherm. Res. Vol. 8, 177-189.

GERLACH, T.M. and GRAEBER, E.J. (1985): Volatile budget of Kilauea volcano. Nature, Vol. 313, 273-277.

GÈZE, B. (1943): Géographie physique et géologie du Cameroun occidental. Mém. Muséum National d'hist. nat., N. Sér., T. 17/1, 1-271.

GHIORSO, M.S. and CARMICHAEL, I.S.E. (1981): A Fortran IV computer program for evaluating temperatures and oxygen fugacities from the compositions of coexisting iron-titanium oxides. Comput. Geosci. 7, 123-129.

GOLD, T. and SOTER, S. (1980): The deep-earth-gas hypothesis. Scient. Americ. 1980.

GOUHIER, J., NOUGIER, J. and NOUGIER, D. (1974): Contribution à l'étude volcanologique du Cameroun (Ligne du Cameroun-Adamaoua). Ann. de la Fac. Sci. Cameroun, No. 17, 3-48.

HASSERT, K. (1912): Seenstudien in Nord-Kamerun. Ztschr. Ges. Erdkunde, 7-41, 135-144, 203-216, Berlin.

HERVIG, R.L. and SMITH, J.V. (1980): Sodium thermometer for pyroxenes in garnet and spinel lherzolites. Jour. Geol. 88, 337-342.

HERZBERG, C.T. (1978): Pyroxene geothermometry and geobarometry: experimental and thermodynamic evaluation of some subsolidus phase relations involving pyroxenes in the system CaO-MgO-Al_2O_3-SiO_2. Geochim. Cosmochim. Acta. 42, 945-957.

JÉRÉMINE, E. (1943): Contribution à l'étude pétrographique du Cameroun occidental. Mém. Muséum National d'hist. nat., N. Sér., T. 17/1, 273-318.

KRETZ, R. (1982): Transfer and exchange equilibria in a portion of the pyroxene quadrilateral as deduced from natural and experimental data. Geochim. Cosmochim. Acta. 46, 411-421.

KUSAKABE, M., KANARI, S., OHSUMI, T., ARAMAKI, S. and HIRABAYASHI, J. (1987): Geochemistry of Lake Nyos. Conf. Intern. sur la Catastrophe du Lac Nyos, Yaounde, Cameroun, 16-20 March, 1987, Abstract.

LASSERRE, M. (1978): Mise au point sur les granitoïdes dits «ultimes» du Cameroun: gisement,

pétrographie et géochronologie. Bull. B.R.G.M. 2e Sér., Sect. IV, 143–159.
LENSCH, G. (1968): Der normative Mineralbestand von Mafititen. N. Jb. Miner. Mh., 9, 306–320.
LORENZ, V. (1973): On the formation of maars. Bull. Volcanol. 37, 138–204.
LORENZ, V. (1986): On the growth of maars and diatremes and its relevance to the formation of tuff rings. Bull. Volcanol. 48, 265–274.
LORENZ, V. and ZIMANOWSKI, B. (1984): Fragmentation of alkali-basaltic magmas and wall-rocks by explosive volcanism. Ann. Sci. Univ. Clermont-Fd. II, 74, 15–25.
MARECHAL, A. LE (1976): Géologie et géochemie des sources thermominérales du Cameroun. Travaux et Documents de l'OSTROM, No. 59, 176 p., Paris.
MATHEZ, E.A., DIETRICH, V.J. and IRVING, A.J. (1984): The geochemistry of carbon in mantle peridotites. Geochim. Cosmochi. Acta, Vol. 48, 1849–1859.
MATTEY, D.P. (1987): Carbon isotopes in the mantle. TERRA cognita 7, 31–37.
MERCIER, J.-C. (1976): Single pyroxene geothermometer and geobarometer. Am. Mineral. 61, 603–615.
MERILL, R.B. and Wyllie, P.J. (1974): Kaersutite and kaersutite eclogite from Kakanui, New Zealand. Water-excess and water deficient melting to 30 kilobars. Geol. Soc. Am. Bull., 86, 555–570.
MESCH, D. (1916): Die Basalte des Kamerungebirges und des Gebietes zwischen Kamerungebirge und Elefantensee. N. Jb. Mineral. Beilg. Bd. 40, 457–532.
MIYASHIRO, A. (1978): Nature of alkalic volcanic rock series. Contr. Mineral. Petrol., 66, 91–104.
NISBETT, E.G., DIETRICH, V.J. and ESENWEIN, A. (1979): Routine trace element determination in silicate minerals and rocks by X-ray fluorescence. Fortschr. Mineral. 57/2, 264–279.
ÓSKARSSON, N. (1987): Carbon dioxide bursts from Lake Nyos, Cameroun, modelled as periodic supersaturation in countercurrent reactor. Conf. Intern. sur la Catastrophe du Lac Nyos, Yaounde, Cameroun, 16–20 March, 1987, Abstract.
RINGWOOD, A.E. (1975): Composition and petrology of the earth's mantle. McGraw Hill Inc., New York, 618 p.
ROEDER, P.L., CAMPBELL, I.H. and JAMIESON, H.E. (1979): A re-evaluation of the olivine-spinel geothermometer. Contrib. Mineral. Petrol. 68, 325–334.
SACHTLEBEN, TH. and SECK, H.A. (1981): Chemical control of Al-solubility in orthopyroxene and its implications on pyroxene geothermometry. Contrib. Mineral. Petrol. 78, 157–165.
SANO, Y., TOMINAGA, T., NAKAMURA, Y. and WAKITA, H. (1982): $^{3}He/^{4}He$ ratios of methane-rich natural gases in Japan. Geochem. Journ. 16, 237–245.
SATO, M. (1978): Oxygen fugacity of basaltic magmas and the role of gas forming elements. Geophys. Res. Let. Vol. 5, 447–449.
SIGURDSSON, H., DEVINE, F.M., PRESSER, T.S., PRINGLE, M.K.W. and EVANS, W.S. (1986): Origin of the lethal gas burst from Lake Manoun, Cameroon. J. Volcanol. Geotherm. Res. 1986 (in press).
SIXTA, V. (1977): Coulometric determination of carbonates in rock samples. Ztschr. Anal. Chem. 285, 369–372.
STUART, G.W., FAIRHEAD, J.D., DORBATH, L. and DORBATH, C. (1985): A seismic refraction study of the structure associated with the Adamawa plateau and Garoua rift, Cameroon, West Africa. Geophys. J. Roy. Astr. Soc., 81, 1–12.
TCHOUA, F.M. (1983): Les explosions magmatophréatiques de Monoun. Revue Sci. Techn. 3, 87–97.
TIETZE, K. (1987): A possible explanation of the Lake Nyos gas burst, based of a newly discovered special stratification effect. Conf. Intern. sur la Catastrophe du Lac Nyos, Yaounde, Cameroun, 16–20 March, 1987, Abstract.
TUTTLE, M.L., EVANS, W.C. and KLING, G.W. (1987): Geochemistry of Lake Nyos: Implications for the origin and accumulation of carbon dioxide. Conf. Intern. sur la Catastrophe du Lac Nyos, Yaounde, Cameroun, 16–20 March, 1987, Abstract.
VERSCHUREN, J. (1965): Un facteur de mortalité mal connu, l'Asphixie par gaz toxique naturels au parc national Albert, Congo. La Terre et la Vie, No. 3, 215–237.

WASS, S.Y. and ROGERS, N.W. (1980): Mantle metasomatism-precursor to continental alkaline volcanism. Cosmochim. Acta, Vol. 44, 1811–1823.

WELLS, P.R.A. (1977): Pyroxene thermometry in simple and complex systems. Contrib. Mineral. Petrol. 62, 129–139.

WOOD, B.J. and BANNO, S. (1973): Garnet-orthopyroxene and orthopyroxene-clinopyroxene relationships in simple and complex systems. Contrib. Mineral. Petrol. 42, 109–124.

YODER, H.S. JR. and TILLEY, C.C. (1962): Origin of basaltic magmas: an experimental study of natural and synthetic rock systems. J. Petrol., 3, 342–532.

Manuscript received March 10, 1987; revised manuscript accepted April 4, 1987.